

Research

A digital twin framework for real-time healthcare monitoring: leveraging AI and secure systems for enhanced patient outcomes

Ahmed K. Jameil^{1,2} · Hamed Al-Raweshidy¹

Received: 18 September 2024 / Accepted: 24 March 2025

Published online: 09 April 2025

© The Author(s) 2025 [OPEN](#)

Abstract

Digital Twin (DT) technology in healthcare is relatively new and faces several challenges, e.g., real-time data processing, secure system integration, and robust cybersecurity. Despite the growing demand for real-time monitoring frameworks, further improvements remain possible. In this study, an architecture has been introduced that utilises cloud computing to create a DT ecosystem. A group of 20 participants has been monitored continuously using high-speed technology to track key physiological parameters, i.e., diabetes risk factors, heart rate (HR), oxygen saturation (SpO₂) levels, and body temperature (BT). To strengthen the study and enhance diversity, the dataset was supplemented with 1177 anonymized medical records from the publicly available MIMIC-III Public Health Dataset. The DT model functions as a tool, storing both real-time sensor data and historical records, to effectively identify health risks and anomalies. An MLP model was combined with XGBoost, resulting in a 25% reduction in training time and a 33% reduction in testing time. The model demonstrated reliability with an accuracy of 98.9% and achieved real-time accuracy of 95.4%, alongside an F1 score of 0.984. Meticulous attention has been paid to cybersecurity measures, ensuring system integrity through end-to-end encryption and compliance with health data regulations. The incorporation of DT and AI within the healthcare sector is seen as having the potential to overcome existing limitations in monitoring systems, while workloads are relieved and data-driven diagnostics and decision-making processes are improved, e.g., through enhanced real-time patient monitoring and predictive analysis.

Highlights

- A hybrid digital twin framework integrates IoT, AI, and secure systems to enhance real-time healthcare monitoring.
- Achieved 98.9% accuracy in predicting health metrics such as heart rate, oxygen levels, and diabetes risk factors.
- Implements robust cybersecurity and cloud computing to ensure data privacy, scalability, and efficient patient care.

Keywords Healthcare technology · Real-time monitoring · Autocorrelation analysis · Rolling average · MXBoost · End-to-end encryption

✉ Hamed Al-Raweshidy, hamed.al-raweshidy@brunel.ac.uk; Ahmed K. Jameil, 2006957@brunel.ac.uk | ¹College of Engineering, Design and Physical Sciences, Brunel University of London, Uxbridge, Middlesex UB8 3PH, London, UK. ²Department of Computer Engineering, College of Engineering, University of Diyala, New Baqubah, Baqubah 32001, Diyala, Iraq.



1 Introduction

Digital Twin (DT) has emerged as an essential tool in different sectors and has developed rapidly over time. As a dynamic digital replica of physical entities, its applications have been notably successful in engineering and industrial sectors [1–3]. In healthcare, where chronic conditions, e.g., diabetes mellitus (DM), are increasingly prevalent, DT's potential to transform patient health services is becoming an area of focus [4]. This paper aims to explore DT's innovative applications in healthcare, particularly in addressing complex health challenges [5, 6].

Historically, DT has been applied in areas such as aerospace, simulating aerodynamics, and manufacturing to optimise production processes [7, 8]. Its integration with advanced technologies, i.e., IoT, AI, and machine learning (ML), further underscores its versatility [9–11]. However, the adoption of DT in Personal Health Systems (PHS) is still in its nascent stages, with current research primarily focusing on integrating electronic health records (EHR) and IoT devices for real-time monitoring [12, 13].

The rise of Industry 4.0 has enhanced DT's relevance in healthcare by leveraging advanced computational and communication technologies. Despite its potential, implementing DT in healthcare presents challenges, e.g., data integration complexities, privacy concerns, and the need for constant updates [14–17]. The launch of models like VitalSense, designed for remote health monitoring in smart cities, signifies significant progress in healthcare technology. However, integrating numerous technological components and ensuring robust data security remain key challenges, necessitating a comprehensive approach to healthcare innovation [18, 19].

This paper navigates the complex landscape of DT in healthcare by identifying gaps and proposing novel solutions. The contributions of this work are as follows:

1. An architectural design is presented that utilises real-time sensor data for monitoring vital signs—heart rate (HR), oxygen saturation (SpO₂), and body temperature (BT), while combining historical data, real-time analytics, and AI for predictive analysis.
2. The MXBoost hybrid model has been developed, combining XGBoost and Multilayer Perceptron (MLP) to address challenges associated with real-time and historical data analysis.
3. A comprehensive DT model (\mathcal{M}_{DT}) has been designed for healthcare, integrating cloud computing with AI, IoT, and robust cybersecurity to enhance operational efficiency and security. A practical Jupyter Notebook dashboard has also been developed for real-time cost monitoring. Additionally, cost-effective concepts in sensor-assisted data acquisition and telemonitoring are introduced, ensuring that these advancements are feasible in healthcare settings.
4. A novel Autocorrelation Analysis technique has been introduced, improving the identification of temporal correlations in healthcare data and assessing the statistical significance of identified disparities in patient health predictions. This method marks a significant advancement in long-term health trend analysis.
5. A state-of-the-art rolling average approach has been utilised by the model, tested on over 10,000 data points to ensure its effectiveness in managing fluctuating healthcare data. This approach removes biases, maintains uniform forecasts, and improves accuracy and reliability, setting a new standard for future healthcare prognostics.

This paper contributes to the academic discourse on DT in healthcare, providing practical insights with significant societal impact. The structure of the paper is as follows: Sect. 2 reviews the literature on DT in healthcare, Sect. 3 details the proposed DT model architecture, Sect. 4 describes the MXBoost algorithm, Sect. 5 presents real-time analysis through Digital Twin Healthcare (DTH), Sect. 6 discusses evaluation and results, Sect. 7 outlines the methodology and future work, and Sect. 8 concludes the study.

This manuscript employs several technical abbreviations and terminologies frequently used in the domain of DT in healthcare. Table 1 provides a detailed list of all abbreviations used throughout the manuscript.

2 Related work

The concept of Industry 4.0 has had a significant impact across multiple sectors, including healthcare, leading to the development of Healthcare 4.0. This new paradigm is characterised by the integration of automation, digitisation, and intelligent technologies to enhance operational efficiency and patient outcomes [20–24]. Extensive research

Table 1 Abbreviations

| Symbol | Description | Symbol | Description |
|------------------------|---|------------------------|---|
| DT | Digital Twin | DTH | Digital Twin Healthcare |
| IoT | Internet of Things | AI | Artificial Intelligence |
| MLP | Multilayer Perceptron | XGBoost | Extreme Gradient Boosting |
| SpO2 | Oxygen Saturation | HR | Heart Rate |
| BT | Body Temperature | DM | Diabetes Mellitus |
| EHR | Electronic Health Records | MIMIC-III | Medical Information Mart for Intensive Care III |
| PaaS | Platform as a Service | RBAC | Role-Based Access Control |
| HIPAA | Health Insurance Portability and Accountability Act | GDPR | General Data Protection Regulation |
| WBANs | Wireless Body Area Networks | JSON | JavaScript Object Notation |
| MQTT | Message Queuing Telemetry Transport | API | Application Programming Interface |
| \mathcal{M}_{DT} | Digital Twin Model | $\mathcal{D}_C(t)$ | Data Acquired by IoT Hub |
| $\mathcal{B}_{IoT}(t)$ | IoT-Based Gateway for Data | \mathcal{R}_{DT} | Data Transmission Rate |
| D_T | Amount of Data Transmitted | Θ_{trans} | Transmission Time |
| $S_{required}$ | Required Storage Space | GANs | Generative Adversarial Networks |
| TLS | Transport Layer Security | E2EE | End-to-End Encryption |
| δ_{AZH} | Azure IoT Hub Gateway | $\lambda_{PDJ}(d)$ | Pack Data to JSON Function |
| $S_{RMAX30102}$ | Sensor Reading for MAX30102 | $S_{RMLX90614}$ | Sensor Reading for MLX90614 |
| \mathcal{RT}_d | Real-Time Data | \mathcal{HB}_p | Historical Behavior Pattern |
| \mathcal{HP} | Historical Pattern Data | \mathcal{RTP} | Real-Time Pattern |
| DoS | Denial-of-Service | CIA | Confidentiality, Integrity, Availability |
| \mathcal{P}_{data} | Patient Information | \mathcal{P}_{policy} | Policy Details |
| \mathcal{P}_{id} | Patient Unique Identifier | Θ_{DEHR} | Secure Data Transmission to EHR |
| \mathcal{R}_{EHR} | Response from EHR | Λ_{DMHIS} | Data Mapping for HIS |
| \mathcal{M}_{data} | Mapped Patient Data | R | User Roles |
| P | Permissions | ΔV | Data Volume |
| ΔD | System Demand | \mathcal{B} | Backup Access |
| Ξ | Scaled System Resources | Ω | Balanced Data Processing |
| Ψ | Backup Service Status | Γ_{SDP} | Adjust Processing Units |
| Λ_{LBD} | Load Balance Data | \mathcal{L} | Load Balancer |
| \mathcal{N} | Node for Data Processing | Σ_{RFT} | Redundancy and Fault Tolerance |
| \mathcal{B}_s | Backup Service | Φ_{DCC} | Dynamic Cloud Capacity |
| Υ_{high} | Upper Threshold for System Demand | Υ_{low} | Lower Threshold for System Demand |
| Θ_{DR} | Disaster Recovery | \mathcal{B}_d | Latest Backup |
| ρ | Down-scaling Parameter | σ | Up-scaling Parameter |
| $D_{historical}$ | Historical Dataset | α | Statistical Confidence Interval |
| N | Total Number of Occurrences | r_k | Autocorrelation at Lag k |

has focused on the integration of DT and IoT in healthcare [25]. In a study by Sarp et al. [26], a DT model integrated with AI was developed for chronic wound management, emphasising personalised treatments and real-time tracking capabilities. However, its application in resource-poor settings may be constrained by the need for consistent data collection and advanced technologies. Elayan et al. proposed a theoretical framework combining IoT devices with edge computing to improve the delivery of healthcare data [25].

Liu et al. explored innovative DT applications for improving elderly healthcare services [27]. Menon et al. analysed virtual copies of patient anatomical structures for personalised therapies [28]. Furthermore, Jia et al. examined enhanced methodologies for constructing DTs [29]. Das et al. focused on the potential of DT and IoT in digital healthcare, particularly in surgical advancements [30]. Corral-Acero et al. and Zhang et al. explored DT applications in specialised medical fields, e.g., cardiology and lung cancer treatment [31, 32]. These studies highlight the transformative potential of DT and IoT in healthcare, while also indicating that the field remains in its early stages.

Research has also explored the application of machine learning (ML) algorithms and sensor technologies in healthcare [33–36]. Panahi et al. discussed the integration of wearable sensors with ML technology for personalised healthcare [37]. Rajesh and Dhuli presented a methodology employing resampling techniques with the AdaBoost ensemble classifier for heartbeat classification [38]. Mondéjar-Guerra et al. validated the effectiveness of ensemble classifiers for heartbeat classification [39]. Research in [40, 41] proposed an AI model for personalised diets in managing genetic predispositions to diabetes, focusing on individualised nutritional recommendations. Additionally, advancements in clustering techniques have enabled the identification of obesity-related patterns in health survey data, with lifestyle factors being key in differentiating subgroups [42]. While these approaches assist in guiding healthcare interventions, they risk oversimplifying the multifaceted nature of obesity, possibly leading to less effective treatments.

Despite these advancements, significant challenges remain in the healthcare sector regarding the implementation of these technologies. Kocabas et al. concentrated on data privacy and security concerns [43]. Further research has highlighted significant progress alongside the challenges inherent in healthcare technology [44, 45]. An essential component of these advancements is the incorporation of blockchain technology to enhance the security and confidentiality of healthcare data systems, which is crucial for the effectiveness of digital therapeutics [46, 47].

Hajar et al. discussed the applications and challenges of wireless body area networks (WBANs) [48]. Aghdam et al. analysed the transformational potential and challenges associated with the implementation of IoT in healthcare [49]. These studies underscore the need to address challenges such as data privacy, security, and real-time data integration to fully realise the potential of these technologies in healthcare. A summary of key contributions from the literature is provided in Table 2, categorising studies based on their scope, data sources, real-time capabilities, limitations, and practical implementations. This table serves as a quick reference for understanding the state-of-the-art in DT healthcare, highlighting the gaps this work seeks to address.

Our research aims to bridge these gaps. Unlike previous studies, this work introduces a novel hybrid algorithm that integrates physical devices with digital models for real-time health monitoring. Cloud computing has been leveraged for data storage, and a Jupyter Notebook dashboard has been employed for efficient data analysis. This approach improves the practicality and usability of the system, particularly within healthcare contexts. Additionally, the framework offers economic efficiency, reinforcing the feasibility and viability of the proposed solution.

Table 2 Overview of DT healthcare applications

| Ref. no | Scope | RTC ^a | RWD ^b | Limitations | Practical work |
|----------|-------------------------|------------------|--|----------------------------|----------------------------------|
| [50] | Healthcare | Yes | Case Studies | Accuracy, latency | VR DT cloud infrastructure |
| [46] | IIoT | Yes | External RT Data | Data collaboration | Experiments, simulations |
| [27] | Healthcare | Yes | Wearable RT Data | Data transfer technology | Hospital ward simulation |
| [29] | IIoT | Yes | Multi-attribute RT Data | Scalability, complexity | Multi-attribute resampling |
| [40] | PFD ^c | N/A | Product Data | NN predictions, safety | Dietary response analysis |
| [41] | Healthcare | Yes | Clinical Data | Resource scarcity | Clinical analysis |
| [25] | SHC ^d | Yes | ECG Data | Data link issues | Context-aware system |
| [26] | Chronic Wound Care | N/A | Clinical Images | Security, interoperability | Camera imaging, segmentation |
| [44] | SDHC ^e | Yes | People Flow Data | Security, privacy | Context-aware system |
| [45] | Diabetes Mgmt. | N/A | Glucose Time Series | Glucose stability | Glucose patient data |
| [33] | Elderly Type-2 Diabetes | Yes | CGM, Insulin Pump Data | Personalization | Pilot studies, real-world setups |
| [34] | WT ^f | Real-world Data | Yes | Interactivity, accuracy | HW-SW integration |
| [9] | Healthcare | Yes | Simulated + Real Data | Glucose simulation | DT glucose simulation |
| Our work | Healthcare | Yes | External RT Data (Glucose, HR, SpO2, BT) | Sensor integration | AI-based RT monitoring |

^a Real-time case study

^b Real-world data

^c Personalized food & diabetes

^d Smart healthcare

^e Social distancing in healthcare

^f Wearable technology

3 Proposed architecture

3.1 System overview

The healthcare monitoring system utilises DT technology to enhance patient monitoring, diagnosis, and real-time intervention. In this study, 20 participants were selected, balancing the need for detailed insights with practical limitations. This selection aligns with the recommendation in [51] to determine sample size based on the study's context and objectives. To enhance the diversity and robustness of the analysis, the dataset was supplemented with 1177 anonymised medical records from the publicly available MIMIC-III Public Health Dataset. This hybrid approach ensures the system is evaluated across a wide range of demographics and healthcare scenarios.

The system's foundation comprises a reliable network of sensors, including the NodeMCU ESP8266 microcontroller, Max30102 heart rate and blood oxygen sensor, and the MLX90614 infrared thermometer. These sensors continuously collect health data, transmitting it securely, as shown in Fig. 1. The collected data is processed in the Microsoft Azure Cloud infrastructure, where artificial intelligence (AI) models generate dynamic, predictive health insights to detect patterns and potential risks.

Within the DT model, the physical and digital realms influence each other, ensuring that changes in one are reflected in the other, thereby maintaining accuracy and relevance. Healthcare professionals can easily access patient data, identify trends, and detect health concerns via the system's dashboard, improving the efficiency of remote patient monitoring. The platform employs advanced AI to reduce healthcare costs and enhance patient care, providing accessible data to both rural and densely populated healthcare areas. The system enables real-time monitoring, predictive analysis, and preventive therapies, supported by robust cybersecurity and a user-friendly visualisation interface.

3.2 IoT devices

The proposed design incorporates IoT devices equipped with various sensors, which serve as essential data collection points for monitoring key health indicators, including HR, SpO₂, and BT. These sensors, selected for their robustness and accuracy, play a vital role in ensuring reliable data acquisition for healthcare monitoring, as demonstrated in similar use cases [34, 52].

The IoT-based health monitoring system utilises an asynchronous communication model, leveraging the publish/subscribe method inherent in the MQTT protocol. The system logs indicate that IoT nodes periodically transmit telemetry data, such as HR, SpO₂, and BT readings, to the cloud. Each data transmission is timestamped to ensure

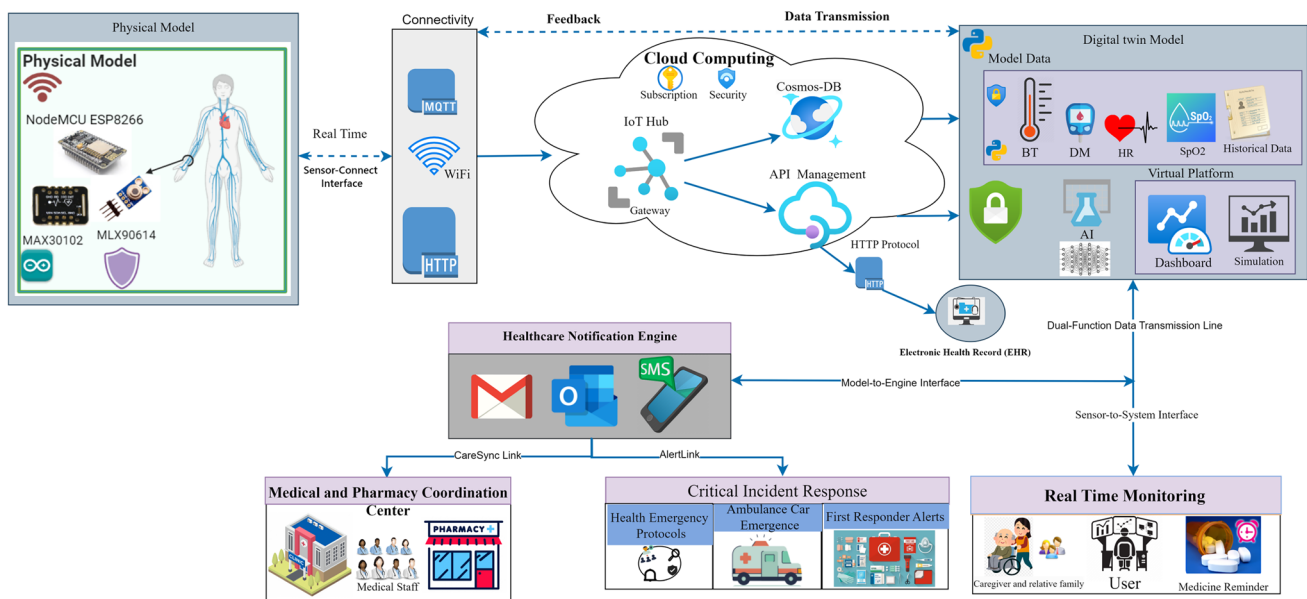


Fig. 1 Architecture of healthcare digital twin based on cloud

a non-blocking, efficient sequence of operations. The data packets are subsequently published as JSON objects to designated cloud endpoints, enabling further processing and analysis. This design highlights the system's capacity to handle high-frequency data from multiple IoT devices simultaneously, optimising cloud communication for scalability and real-time responsiveness in DTH applications, as depicted in Fig. 2.

Figure 2a illustrates the interconnection of the NodeMCU ESP8266, MLX90614, and MAX30102 sensors within the system. Figure 2b demonstrates the transfer of data from physical devices to cloud storage, showcasing the system's secure and efficient data transmission capabilities. Figure 2c displays live sensor data on an Arduino monitor, while Fig. 2d presents a simulation of the physical system in the cloud-based \mathcal{M}_{DT} , involving data transmission to the Azure IoT Hub.

Algorithm 1 outlines a systematic process for data collection and transmission within the IoT-based healthcare system. The initial setup involves creating a wireless network connection and configuring the sensor interfaces. The system then continuously collects data from the health monitoring sensors, structures it in JSON format, and transmits it to multiple destinations. These destinations include an API for data processing, a dashboard for data visualisation, and \mathcal{M}_{DT} , ensuring comprehensive management of health data and efficient analysis.

Algorithm 1 Data transfer and acquisition using the IoT device

```

Input:  $\omega_{\text{conn}}$ (ssid, password), Device Key
Output:  $\delta_{\text{AZH}}, \mathcal{D}_B, \mathcal{M}_{DT}$ 
1: procedure  $\mathcal{I}_{\text{init}}$  # Initialise is  $\mathcal{I}_{\text{init}}$ 
2:  $\omega_{\text{conn}}$ (ssid, password), Device Key # Connect to WIFI step
3:  $\mathcal{I}_{\text{init}} \leftarrow \text{Sensors}()$ 
4:  $\mathcal{I}_{\text{init}} \leftarrow \delta_{\text{AZH}}$  # Initialise Azure IoT Hub
5: end procedure
6: procedure  $\lambda_{\text{ML}}$  # main Loop
7:   while  $\tau$  do
8:   if  $\Theta_{\text{ST}}$  then # Time to send telemetry is  $\Theta_{\text{ST}}$ 
9:      $d \leftarrow \alpha_{\text{CSD}}$  # Collect sensor data is  $\alpha_{\text{CSD}}$ 
10:     $\delta_{\text{AZH}}(d)$  # Send data to Azure IoT Hub gateway is  $\delta_{\text{AZH}}$ 
11:   end if
12:    $\xi_{\text{MCL}}()$  # MQTT Client Loop function is  $\xi_{\text{MCL}}$ 
13: end while
14: end procedure
15: procedure  $\alpha_{\text{CSD}}$ 
16:   HR, SpO2  $\leftarrow \mathcal{S}_{\text{RMAX30102}}$  # Read data from sensor MAX30102()
17:   BT  $\leftarrow \mathcal{S}_{\text{RMLX90614}}$  # Read data from sensor MLX90614()
18:   return (HR, SpO2, BT)
19: end procedure
20: procedure  $\delta_{\text{AZH}}(d)$ 
21:    $\lambda_{\text{PDJ}}(d)$  # Pack data to JSON(data)
22:    $\delta_{\text{AZH}} \leftarrow \lambda_{\text{PDJ}}(d)$ 
23:    $\mathcal{M}_{\text{API}} \leftarrow \delta_{\text{AZH}}$  # Send data from IoT Hub gateway to API Management.
24:    $\mathcal{D}_B \leftarrow \delta_{\text{AZH}}$  # Send data from IoT Hub gateway to Dashboard.
25:    $\mathcal{M}_{\text{DT}} \leftarrow \delta_{\text{AZH}}$  # Send data from IoT Hub gateway to DT Model
26: end procedure

```

3.3 Cloud computing infrastructure

The cloud platform is employed to model DT through the use of Platform as a Service (PaaS). The PaaS architecture has been specifically tailored for DTH applications, providing a cost-effective and practical solution for handling complex healthcare data. The cloud-based IoT Hub is responsible for receiving and transmitting data collected from IoT devices, ensuring secure and efficient data flow, which is essential in healthcare contexts.

$$\mathcal{D}_C(t) : \mathcal{S}_r(t) \rightarrow \mathcal{B}_{\text{IoT}}(t) \quad (1)$$

The equation above defines a data collection function, $\mathcal{D}_C(t)$, representing the data acquired by the IoT Hub at time t . This function underscores the system's real-time data collection capabilities, which are essential for maintaining the responsiveness of the DT model. The management of data latency, i.e., the reduction of transmission delays, and the assurance of timely processing are facilitated by the component $\mathcal{B}_{\text{IoT}}(t)$, which plays an essential role in the system's performance.

$$\mathcal{R}_{DT} = \frac{D_T}{\Theta_{trans}}, \tag{2}$$

where \mathcal{R}_{DT} , D_T , and Θ_{trans} represent the data transmission rate, amount of data transmitted, and transmission time, respectively. The necessity for optimised transmission rate is highlighted, ensuring the system's efficiency and reliability in real-time health monitoring, e.g., for continuous patient data transmission.

1. Scalable and secure cloud storage systems enable the persistent storage of raw sensor data and health indicators, such as HR, SpO2, and BT. By scaling storage capacity to accommodate patient data growth, the system addresses the challenges posed by digital healthcare.
2. Compliance with healthcare regulations and modern security protocols ensures data security and adherence to legal requirements. These measures safeguard critical health data, while the system's extensive monitoring network enables accurate storage capacity estimation for patient records, as shown in Eq.(3).

$$S_{required} = N \cdot D_v \cdot T \tag{3}$$

In this equation, $S_{required}$ denotes the required storage space, with N representing the total number of patients, D_v the average data generated per patient per unit time, and T indicating the storage duration.

3.4 Security and privacy design in healthcare surveillance systems

The healthcare surveillance system has been carefully designed to ensure the highest standard of security, safeguarding the confidentiality, integrity, and availability (CIA) of patient data. These core security principles are crucial for protecting sensitive healthcare information. The integrated security framework is fully aligned with healthcare data regulations, including the Health Insurance Portability and Accountability Act (HIPAA) and the General Data Protection Regulation (GDPR), ensuring compliance while providing a strong defence against emerging threats.

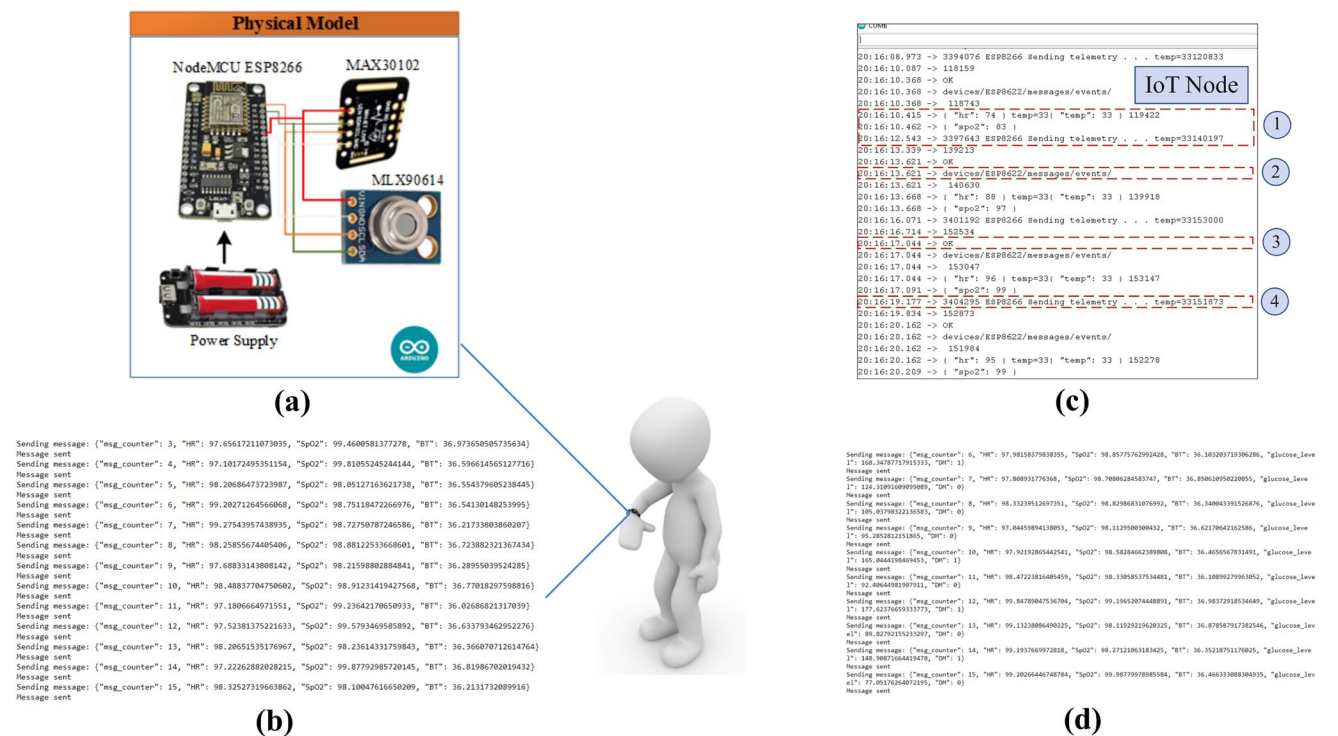


Fig. 2 Schematic representation of data flow from sensors to cloud-based M_{DT} ; **(a)** Sensor configuration. **(b)** Transmission from physical device to cloud. **(c)** Arduino monitor data read. **(d)** Cloud-based M_{DT}

3.4.1 Encryption and data integrity

For secure data transmission, RSA encryption is employed, as outlined in Algorithm 2. This method ensures that data remains confidential when transmitted over HTTPS channels. The integrity of data is rigorously maintained through cryptographic hashing and digital signatures, establishing a verifiable trust chain from the data's origin to its intended destination. The following formalisation encapsulates this process:

$$\mathcal{E}_K(D) \rightarrow \mathcal{C}, \quad (4)$$

[53] the encryption function $\mathcal{E}_K(D)$, is defined as the process of transforming plaintext data D using a cryptographic key K to generate the corresponding ciphertext \mathcal{C} . This procedure ensures the preservation of data confidentiality when transmitted over networks that may be susceptible to security breaches. The integrity of transmitted data and the authentication of its origin are verified through the use of cryptographic hashes and digital signatures.

$$\mathcal{H}(D) \rightarrow H', \quad (5)$$

[54] in this case, $\mathcal{H}(D)$ denotes the hash function, which is responsible for transforming the input data D into the resulting hash value H' .

Algorithm 2 Secure data transmission with multi-layered security

```

1: Input:  $\mathcal{D}, \mathcal{K}_{pubR}, \mathcal{K}_{priS}$  # Input data  $\mathcal{D}$  to transmit,  $\mathcal{K}_{pubR}$  is receiver's public key, and  $\mathcal{K}_{priS}$  is
   sender's private key.
2: Output:  $\mathcal{T}_{secure}$  # Output is secure data transmission confirmation.
3:  $\mathcal{E} \leftarrow \text{Encrypt}(\mathcal{D}, \mathcal{K}_{pubR})$  #  $\mathcal{E}$ : Encrypted data.
4:  $\mathcal{H} \leftarrow \text{CalculateHash}(\mathcal{D})$  #  $\mathcal{H}$ : Hash of original data.
5:  $\mathcal{S} \leftarrow \text{Sign}(\mathcal{D}, \mathcal{K}_{priS})$  #  $\mathcal{S}$ : Signature of the data.
6:  $\mathcal{C} \leftarrow \text{ISC}()$  # Initiate secure channel is ISC,  $\mathcal{C}$  is secure communication channel (TLS, HTTPS).
7:  $\text{Transmit}(\mathcal{E}, \mathcal{S}, \mathcal{C})$  # Transmit encrypted data and signature on secure channel.

8: # Receiver side
9:  $\mathcal{R}, \mathcal{S}_{recv} \leftarrow \text{Receive}(\mathcal{C})$  #  $\mathcal{R}$ : Received data,  $\mathcal{S}_{recv}$ : Received signature.
10:  $\mathcal{D}_{dec} \leftarrow \text{Decrypt}(\mathcal{R}, \mathcal{K}_{priR})$  #  $\mathcal{D}_{dec}$ : Decrypted data.
11:  $\mathcal{V} \leftarrow \text{VerifySignature}(\mathcal{S}_{recv}, \mathcal{K}_{pubS}, \mathcal{D}_{dec})$  #  $\mathcal{V}$ : Signature validation flag.
12: if  $\neg \mathcal{V}$  then
13:   raise AuthenticationError # Signature verification failed.
14: else
15:    $\mathcal{H}_{recv} \leftarrow \text{CalculateHash}(\mathcal{D}_{dec})$  #  $\mathcal{H}_{recv}$ : Recalculated hash of decrypted data.
16:   if  $\mathcal{H}_{recv} \neq \mathcal{H}$  then
17:     raise IntegrityError # Data integrity is compromised
18:   else
19:     Success! Data transmitted securely and verified
20:   end if
21: end if

```

3.4.2 Access control and anomaly detection in DT model

The \mathcal{M}_{DT} system uses a robust role-based access control (RBAC) framework to protect patient information, meeting regulatory requirements and assigning access rights appropriately. User roles are linked to specific permissions, and ensuring that patient data is accessible only to authorised staff is expressed by the following equation:

$$\mathcal{AC}(U, R) \rightarrow P, \quad (6)$$

where \mathcal{AC} represents the access control mechanism, U denotes the user, R refers to the assigned role, and P specifies the permissions. Regular reviews and updates of user roles (R) and permissions (P) ensure that access aligns with job responsibilities, thereby maintaining both security and operational efficiency.

To further enhance security, the \mathcal{M}_{DT} system integrates an advanced anomaly detection algorithm, as detailed in Algorithm 3. This algorithm effectively identifies and addresses potential threats by detecting unusual patterns, ensuring the integrity and availability of the system.

Algorithm 3 Anomaly detection in digital twin model

```

1: Input:  $\mathcal{RT}_d, \mathcal{HB}_p$  #  $\mathcal{RT}_d$  is real-time data,  $\mathcal{HB}_p$  is historical behaviour pattern.
2: Output:  $AD_r$  # Anomaly detection report.
3:  $\mathcal{HP} \leftarrow \text{LoadHistoricalPattern}(\mathcal{HB}_p)$  #  $\mathcal{HP}$ : Historical pattern data.
4:  $\mathcal{RTP} \leftarrow \text{ExtractPattern}(\mathcal{RT}_d)$  #  $\mathcal{RTP}$ : Extracted real-time pattern.
5:  $AD_r \leftarrow \text{ComparePatterns}(\mathcal{HP}, \mathcal{RTP})$  # Compare historical and real-time patterns for anomalies.
6: if  $AD_r$  indicates an anomaly then
7:    $\text{TriggerSecurityProtocol}()$  # Anomaly detected; take precautions.
8: end if

```

3.4.3 Visualisation of the security framework

In Fig. 3, the multi-layered security framework of the healthcare monitoring system is illustrated, showing the various security protocols that are implemented across different levels. This visualisation demonstrates how patient data is protected comprehensively.

1. Physical layer attacks:

- **Tampering and Device Hijacking:** Unauthorized physical access to IoT devices poses risks such as manipulation of sensor data or the hijacking of devices. To mitigate these threats, the framework integrates secure boot mechanisms, encrypted storage solutions, and stringent physical access safeguards.

2. Network layer attacks:

- **Spoofing** occurs when an attacker impersonates a legitimate device to intercept or disrupt communication. To block unauthorised access, secure methods like TLS and token-based authentication are employed.
- **Eavesdropping and packet sniffing** involve intercepting sensitive information without authorization. To counter these threats, the framework utilises end-to-end encryption and implements network segmentation for enhanced security.

3. Cloud layer attacks:

- **Denial-of-Service (DoS)** attacks occur when malicious individuals flood cloud services with excessive traffic, rendering them inaccessible to legitimate users. To address this issue, the framework incorporates auto-scaling of cloud resources and DDoS protection strategies.
- **Data exfiltration** refers to the unauthorised extraction of sensitive information from cloud systems. To safeguard data integrity and confidentiality, measures such as multi-factor authentication, role-based access controls, and ongoing monitoring are implemented.

4. IoT and DT layer attacks:

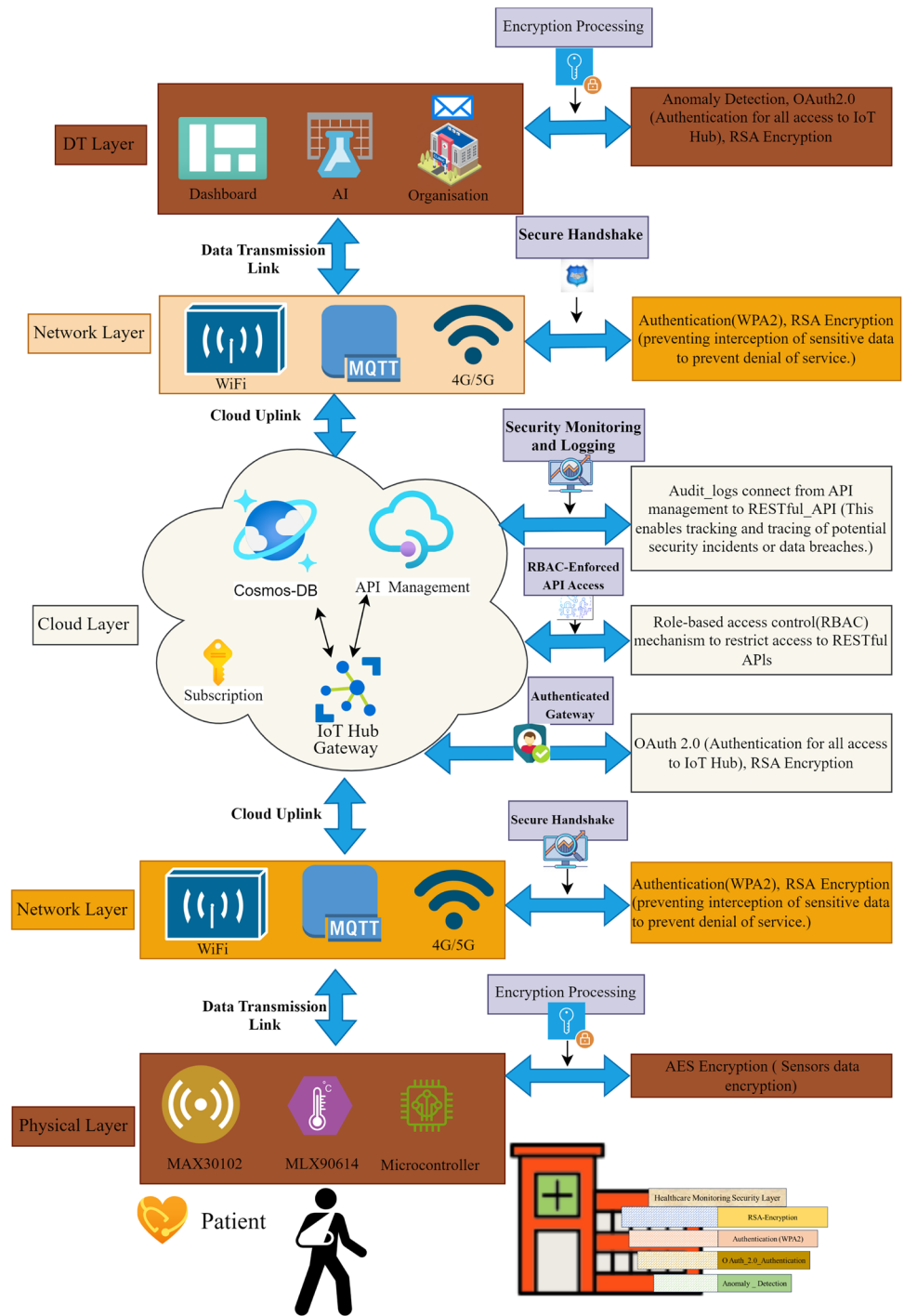
- **Data poisoning** occurs when inaccurate or malicious information is introduced into IoT devices or digital twins, potentially compromising healthcare decisions. To combat this, the framework utilizes anomaly detection algorithms.
- **Firmware tampering**, which involves targeting the firmware of IoT devices, can disrupt system operations. To counter this, the framework relies on routine firmware updates and integrity verification processes.

The outlined threats and their associated security measures are concisely presented in Tables 3 and 4, with further reinforcement provided by the framework's integrated components detailed in Algorithm 4. By targeting vulnerabilities across all layers-physical, network, cloud, and IoT/DT-the proposed security framework delivers comprehensive protection against a wide range of attack vectors.

3.4.4 Assessment of potential threats

A clear understanding of potential threats is crucial for mitigating them and establishing a secure structure. We conducted a comprehensive risk assessment to identify and prepare for various threat vectors, as detailed in Tables 3 and 4.

Fig. 3 Ontology framework for healthcare digital twin cybersecurity



These tables classify common security risks, outline their objectives, and detail their impact on the CIA (Confidentiality, Integrity, and Availability) triad, ensuring that the implemented security measures remain adaptive and responsive to the evolving threat landscape.

Thus, the further development of our security framework encompasses encryption, authentication, access control and monitoring for suspicious activity serve to strengthen our view that healthcare surveillance systems, at the very least, should follow standard security protocols.

Table 3 Classification of cyber threats and effects on DTH security

| Cyber threat aim | Impact on security measures |
|-------------------|--|
| Data access | Confidentiality [55] |
| Data modification | Integrity [55] |
| Data destruction | Confidentiality, integrity |
| Denial of service | Availability [55] |
| System disruption | Availability |
| Ransomware | Confidentiality, integrity, availability[56] |

3.5 Connectivity to healthcare infrastructure

The proposed framework can be used individually or integrated into other structures within healthcare data institutions, with a high priority on data utilisation and incorporation. Algorithm 4 serves as the foundation for this approach, prioritising continuous and seamless connectivity to healthcare systems while ensuring flexibility and compliance with healthcare specifications, including FHIR and HL7.

This algorithm serves as a pivotal component, offering a comprehensive approach for the secure and efficient handling, transmission, and processing of patient data within healthcare systems. It begins by capturing key inputs: \mathcal{P}_{data} , representing the patient's information; \mathcal{P}_{policy} , which outlines relevant policy details; and \mathcal{P}_{id} , the patient's unique identifier. Following the initial input, Θ_{DEHR} ensures the secure transmission of patient data to the EHR system, awaiting a confirmation response, \mathcal{R}_{EHR} , upon successful completion.

Subsequently, the module Λ_{DMHIS} transforms the patient data into \mathcal{M}_{data} , a format optimized for compatibility, thereby facilitating seamless information sharing across diverse healthcare systems. This algorithm not only returns the updated access policy but also consolidates responses from both the EHR and HIS systems. The incorporation of standardized APIs and advanced mapping techniques further enhances the integration process, enabling secure, flexible data management across healthcare infrastructures.

Algorithm 4 Unified patient data management

```

1: Input:  $\mathcal{P}_{data}, \mathcal{P}_{policy}, \mathcal{P}_{id}$  #  $\mathcal{P}_{data}$ =Patient data,  $\mathcal{P}_{policy}$ =Policy details,  $\mathcal{P}_{id}$ =Patient ID.
2: Output:  $\mathcal{R}_{EHR}, \mathcal{R}_{HIS}, \mathcal{S}_{policy}$  #  $\mathcal{R}_{EHR}$ =Response from EHR,  $\mathcal{R}_{HIS}$ =Response from HIS,
    $\mathcal{S}_{policy}$ =Shared access policy.
3: procedure  $\Gamma_{SAP}$  #  $\Gamma_{SAP}$ : Shared Access Policy Creation.
4:    $\mathcal{S}_{policy} = \text{NewPolicy}(\mathcal{P}_{policy})$  # Create new policy.
5:    $\text{SetPermissions}(\mathcal{S}_{policy}, \text{Permissions})$  # Define access permissions.
6: end procedure
7: procedure  $\Theta_{DEHR}$  #  $\Theta_{DEHR}$ : Secure Data Transmission to EHR.
8:    $\mathcal{E}_{endpoint} = \text{GetEndpoint}(\mathcal{P}_{id})$  # Fetch EHR API endpoint
9:    $\mathcal{R}_{EHR} = \text{SendData}(\mathcal{E}_{endpoint}, \mathcal{P}_{data})$  # Transmit data to EHR
10: end procedure
11: procedure  $\Omega_{IWHIS}$  #  $\Omega_{IWHIS}$ : Integrate with HIS.
12:    $\mathcal{H}_{data} = \text{FormatForHIS}(\mathcal{P}_{data})$  # Format data for HIS
13:    $\mathcal{R}_{HIS} = \text{TransferToHIS}(\mathcal{H}_{data})$  # Send to HIS
14: end procedure
15: procedure  $\Lambda_{DMHIS}$  #  $\Lambda_{DMHIS}$ : Data Mapping for HIS.
16:    $\mathcal{M}_{data} = \{\}$  # Initialize mapped data container.
17:   for (key, value) in  $\mathcal{P}_{data}.\text{items}()$ 
18:      $\mathcal{M}_{data}[\text{MapKey}(\text{key})] = \text{MapValue}(\text{value})$  # Map each data item.
19:   end for
20: end procedure
21: return  $\mathcal{R}_{EHR}, \mathcal{R}_{HIS}, \mathcal{S}_{policy}$ 

```

3.6 Scalability and fault tolerance

The efficiency of healthcare systems is dependent on the strength of scalability and fault tolerance in managing patient data and maintaining uninterrupted service. These requirements are addressed by Algorithm 5, which implements reactive scaling in the cloud by dynamically adjusting resource allocation based on real-time data requests. Future developments in proactive scaling, which rely on previous data patterns, are also recognised.

Table 4 Attack objectives and their impact on confidentiality, integrity, and availability

| Layer | Attack type | Attack objective | C | I | A | Vulnerability |
|----------------|-------------------------|--|---|---|---|--|
| Physical layer | Tampering | Unauthorised access to or modification of sensor data | H | M | H | Weak physical security measures, compromised access control, faulty hardware |
| Network layer | Spoofing | Disguising as a legitimate device to gain unauthorized access or disrupt device-to-cloud communication | M | H | M | Unsecured Wi-Fi connections, weak authentication protocols, firmware vulnerabilities |
| Cloud layer | Denial of service (DoS) | Overwhelm cloud services with traffic, making them unavailable for legitimate users | L | L | H | Insufficient service scaling capabilities, unmitigated DDoS vulnerabilities |
| DT layer | Data exfiltration | Extracting Sensitive Data from Digital Twin Services | H | H | L | Inadequate data handling policies, insufficient access controls, lack of monitoring |

H = High

L = Low

M = Medium

Algorithm 5 further outlines methods for managing cloud resources dynamically, including both horizontal and vertical scaling, to accommodate the varying demands of healthcare data processing. The Γ_{SDP} algorithm efficiently handles large data volumes by adjusting processing capacity (Ξ) dynamically, based on the data received (ΔV). When data volumes exceed a predefined threshold (Θ), additional processing units are deployed, ensuring optimal resource usage for varying data loads.

The management of data distribution across multiple processing nodes (\mathcal{N}) is primarily facilitated by the load balancing component, symbolised as Λ_{LBD} , which holds significant importance in system functionality. The deployment of a sophisticated load (\mathcal{L}), the allocation of workloads is enhanced, and enhancement in system efficacy (Ω). Also, extra stratum of robustness is established through the incorporation of Σ_{RFT} , guaranteeing that the system is stable of maintaining uninterrupted operations. This methodology ensures both the integrity and functionality of the system, even amidst challenging circumstances. The provision of availability and fault tolerance within sensitive healthcare settings is reinforced by the backup service (Ψ), whose operational role is paramount and meticulously adjusted in accordance with variations in instantaneous demand (ΔD). The capacity of the cloud is additionally enhanced by (Υ_{high} and Υ_{low}), in conjunction with the precise calibration of resource allocation (ρ), in this case will fostering increased efficiency while concurrently mitigating expenditures. Collectively, these improvements substantially enhance the operational efficacy of Digital Twin Healthcare (DTH) systems, as delineated in Algorithm 5.

Algorithm 5 Resilient and scalable DTH system optimisation

```

1: Input:  $\Delta V$  (Data Volume),  $\Delta D$  (System Demand),  $\mathcal{B}$  (Backup Access)
2: Output:  $\Xi$  (Scaled System Resources),  $\Omega$  (Balanced Data Processing),  $\Psi$  (Backup Service Status)
3: procedure  $\Gamma_{SDP}$  #  $\Gamma_{SDP}$ : Adjust Processing Units
4: if ( $\Delta V > \Theta$ ) then
5:   increase_units( $\delta$ )
6: else
7:   decrease_units( $\epsilon$ )
8: end if
9: end procedure
10: procedure  $\Lambda_{LBD}$  #  $\Lambda_{LBD}$ : Load Balance Data
11:  $\mathcal{L} \leftarrow$  get_load_balancer()
12:  $\mathcal{N} \leftarrow$   $\mathcal{L}$ .select_node()
13:  $\mathcal{N}$ .process( $\Delta V$ )
14: end procedure
15: procedure  $\Sigma_{RFT}$  #  $\Sigma_{RFT}$ : Redundancy and Fault Tolerance
16: if (!service_operational) then
17:    $\mathcal{B}_s \leftarrow$  get_backup()
18:    $\mathcal{B}_s$ .activate()
19: end if
20: end procedure
21: procedure  $\Phi_{DCC}$  #  $\Phi_{DCC}$ : Dynamic Cloud Capacity
22: if ( $\Delta D > \Upsilon_{high}$ ) then #  $\Upsilon_{high}$ ,  $\Upsilon_{low}$ : Upper and Lower Threshold for System Demand
23:   scale_up( $\rho$ ,  $\sigma$ ) #  $\rho$ ,  $\sigma$ : Scale Parameter for Down-, and Up-scaling
24: else if ( $\Delta D < \Upsilon_{low}$ ) then
25:   scale_down( $\rho$ ,  $\sigma$ )
26: end if
27: end procedure
28: procedure  $\Theta_{DR}$  #  $\Theta_{DR}$ : Disaster Recovery
29:  $\mathcal{B}_d \leftarrow$  get_latest_backup()
30: restore_from( $\mathcal{B}_d$ )
31: end procedure

```

4 Hybrid model algorithm

The relevance of health-related variables is evaluated utilising a random forest estimator, which further augments the model's predictive performance. This feature assessment procedure not only improves the model's overall accuracy but also enhances its efficiency relative to conventional MLP and XGBoost frameworks. MXBoost model is the integration of MLP and XGBoost. The architectural framework of the MXBoost model is illustrated in Fig. 3, providing a lucid visual representation of its configuration.

4.1 Data loading and preprocessing

The research uses numerous features and a heavily-imbalanced dataset across all target variables: TargetHR (\mathcal{Y}_{HR}), TargetSpO2 (\mathcal{Y}_{SpO2}), TargetBT (\mathcal{Y}_{BT}), and TargetDM (\mathcal{Y}_{DM}). Advanced imputation methods are used to preserve the quality and reliability of the medical data, ensuring its robustness for model training in future modeling systems and accurate predictions. A wide range of real-time patient sensor data is incorporated with historical datasets, enhancing the model's efficiency and strengthening the dataset to ensure better predictive performance.

In addition to standard performance metrics, a dedicated healthcare analysis was conducted to improve the model's interpretability and deployability in clinical settings. In our study, we utilised the MIMIC-III Public Health Dataset, which contains 1177 medical records from [30], to evaluate performance measures such as accuracy, precision, recall, and F1 score. These metrics are crucial in assessing the model's quality across a variety of healthcare records, providing a detailed evaluation of its applicability to real-world healthcare scenarios.

4.2 Model training and structure

The MLP classifier has been implemented using 100 neurons in one hidden layer for healthcare data classification task. To avoid overfitting and improve the robustness of the model, L2 regularization with Alpha coefficient was used. As shown in Fig. 4, this regularisation term is incorporated into the loss function, which effectively limits the complexity of the model and increases its ability to generalise well across healthcare environments.

Likewise, the XGBoost classifier operating on a gradient boosting foundation has been parameterised with manually predefined $reg_alpha = 0.5$ and $reg_lambda = 2.0$. We tune these parameters to achieve a balance between computational complexity and prediction accuracy. This reduces overfitting risk and makes the model more accurate overall.

4.3 Multi-target classification

Hence, among the multiple clinical measurements are, in SpO2, BT and DM which require to be focused as target variables since they are the most significant ones across the other targets of concern under this multi-output classification scenario. They are crucial to make the model more accurate, useful, and providing a means to effectively predict the important health indicators. Due to healthcare categorisation standards, we transformed columns \mathcal{Y}_{SpO2} , \mathcal{Y}_{BT} , and \mathcal{Y}_{DM} into binary variables switching label 1 to 0 for labels 2,3 or 4 as shown in Algorithm 6.

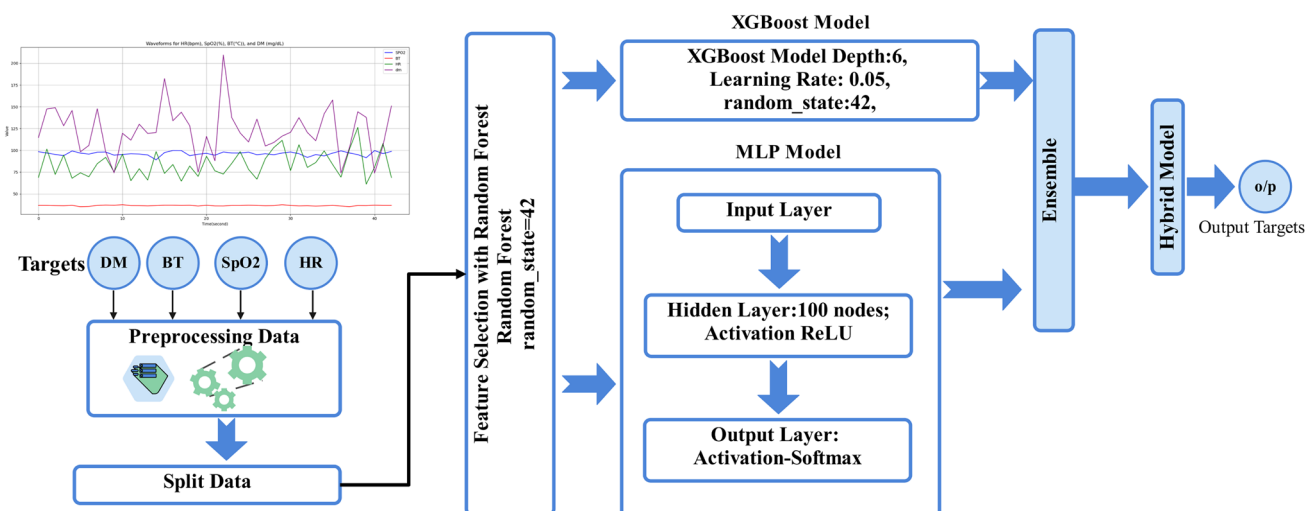


Fig. 4 Hybrid model architecture

Algorithm 6 Pseudo code of data preprocessing

```

1: Input: Load data from historical data
2: Output: Preprocessed data  $X$ 
3: if any missing values in data then
4:   Forward fill missing values
5:   Backward fill remaining missing values
6: end if
7: Replace labels in  $\mathcal{Y}_{SpO_2}$  ( 2  $\rightarrow$  1 )
8: Replace labels in  $\mathcal{Y}_{BT}$  ( 3  $\rightarrow$  1 )
9: Replace labels in  $\mathcal{Y}_{DM}$  ( 4  $\rightarrow$  1 )
10: Set  $X$  as data excluding target columns
11: return  $X$ 

```

The ensemble feature of the MXBoost method utilises predictions from both the MLP and XGBoost models, providing a more comprehensive analysis by accounting for potential misclassifications. Robust performance is thereby ensured when dealing with various types of medical data and supporting decision-making processes.

Robust performance is thereby assured when dealing with multi types of medical data and supporting decision-making processes. The final prediction of the MXBoost model is deduced by calculating the mode of the forecasts generated by both the MLP and XGBoost models, as outlined in Eq.(12).

$$P_{\text{final}} = \text{Mode}(P_{\text{MLP}}, P_{\text{XGB}}), \quad (12)$$

in this environment, the final prediction, denoted as P_{final} , is attained through the integration of the individual prognostications produced by the (P_{MLP}) model P_{mlp} and the XGBoost model (P_{XGB}). This combined approach harnesses the strengths of both models, thereby perfecting the delicacy and trustability of the performing affair.

4.4 Role of AI in real-time diagnosis and prediction

A unique hybrid AI algorithm has been employed within the system for real-time data analysis, specifically developed to identify abnormalities of data and prognosticate health conditions in healthcare settings. The prediction score for diabetes mellitus (P_{DM}) is calculated through a function f , which integrates both real-time health criteria and historical data.

$$P_{\text{DM}} \text{ Score} = f(\text{SpO}_2, \text{HR}, \text{BT}, D_{\text{historical}}) \quad (13)$$

The historical dataset ($D_{\text{historical}}$) has been constructed by incorporating variables such as glucose levels, renal failure, COPD, hypertension, and other pertinent health factors. As a result, more comprehensive and informed forecasting is achieved, particularly in clinical and medical environments.

4.4.1 Anomaly detection threshold

Structural anomalies are determined by analysing both the overall diabetes mellitus prediction score (P) and the historical diabetes mellitus score ($P_{\text{historical}}$). This dual approach allows for a more nuanced detection of irregularities, integrating both current and past data for a comprehensive evaluation. A threshold (θ) is applied to detect significant deviations, as shown below:

$$\text{Anomaly} = \begin{cases} 1, & \text{if } |P - P_{\text{historical}}| > \theta \\ 0, & \text{otherwise.} \end{cases} \quad (14)$$

This threshold is particularly important in the aspect of early detection in a health care setting.

4.4.2 Feedback loop adjustment

The current model parameters (Θ) are adjusted based on the learning rate (α) and the gradient of the loss function ($\nabla L(\Theta)$) to improve predictive performance. The adjustment is governed by the following equation:

$$\Theta' = \Theta - \alpha \cdot \nabla L(\Theta) \quad (15)$$

This feedback loop could help a model improve and update itself very well since it has to work with the most recent data possible.

5 DTH-based real-time analysis and diagnosis

Figure 1 illustrates the data flow and interaction between the components within the DTH architecture. The real-time dashboard serves as an interactive interface, displaying key health metrics retrieved from \mathcal{M}_{DT} . It enables healthcare professionals to monitor patients in real time. The dashboard interacts with an API to obtain metrics such as BT, SpO2, HR, and DM status. Initially, the dashboard presents a set of data, and it continuously updates every two seconds by making API requests. This process ensures that the displayed metrics remain current, as shown in Figs. 5 and 6.

6 Evaluation and results

6.1 Model training and testing time

The empirical data indicate that the training and testing durations for each model were meticulously recorded. For instance, the MLP model assigned to TargetHR required a training time of 6.3140 s, followed by a testing time of 6 milliseconds. The consistently swift testing times across all models, e.g., the MLP and XGBoost models, demonstrate the system’s suitability for real-time applications.

6.2 Model performance

The classification performance of a hybrid model for patient health data, including HR, SpO2, BT, and DM, is illustrated by the confusion matrix heatmap in Fig. 7. Each element within the matrix represents the number of accurate and inaccurate classifications produced by the model. A comprehensive analysis of true positives, false positives, true negatives, and false negatives for each health measure is provided, offering insights into the model’s predictive accuracy and highlighting specific areas where improvements could be made.

The performance characteristics of the prediction models are depicted in Fig. 8, which is divided into two subfigures for clarity. Figure 8a illustrates the performance metrics of the baseline models, where each axis represents a performance

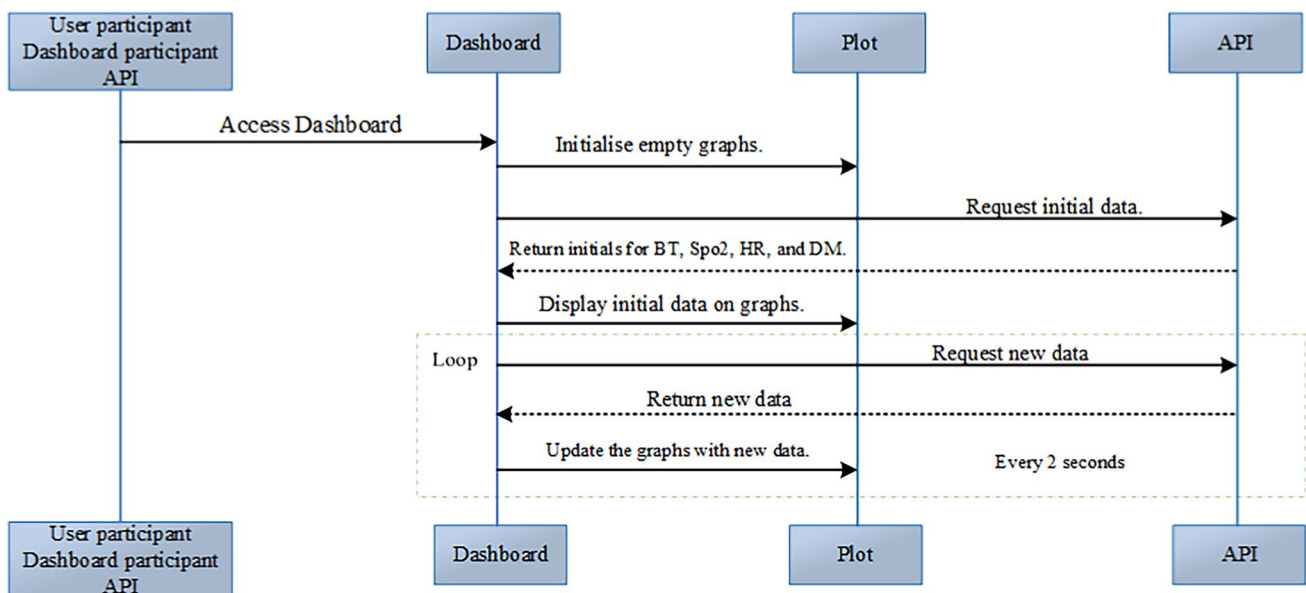


Fig. 5 Sequence diagram illustrating real-time data flow within the dashboard

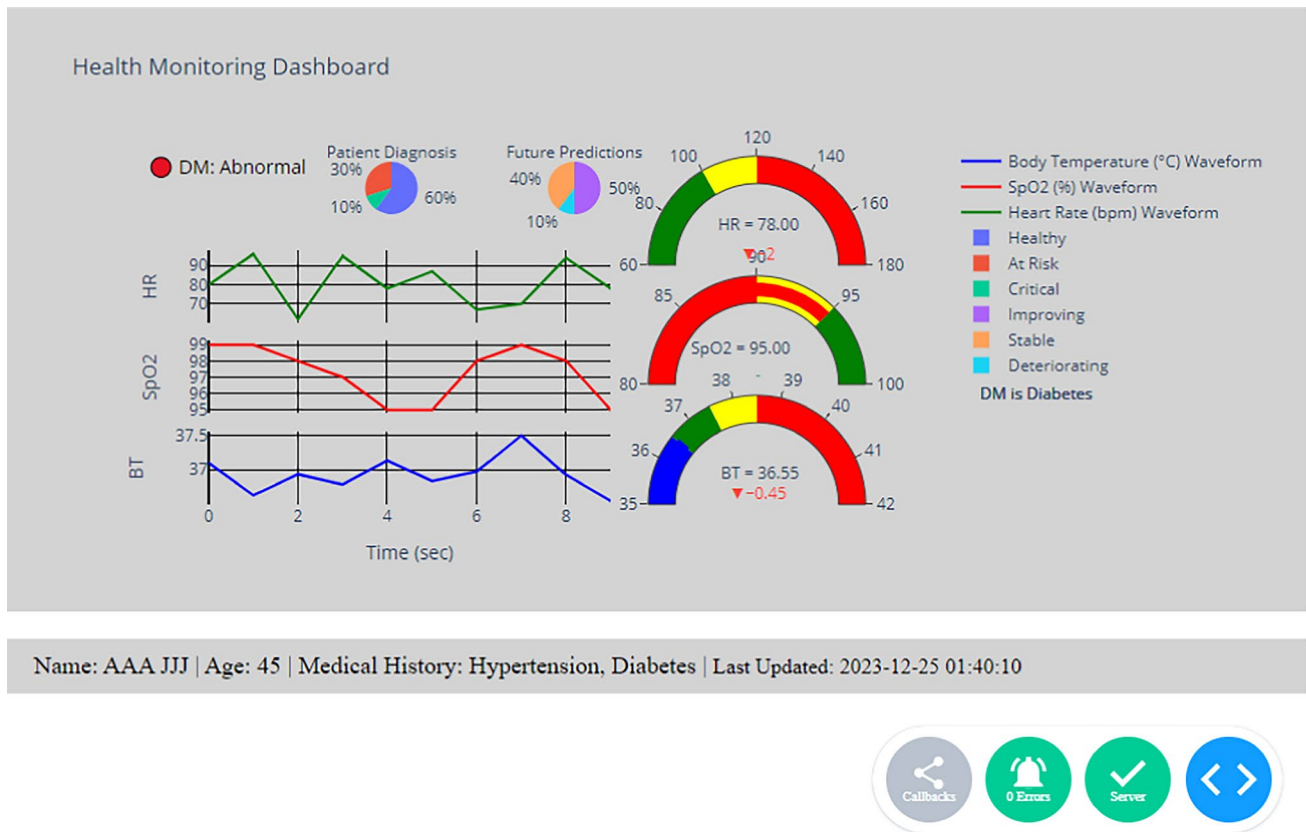


Fig. 6 Real-time patient monitoring dashboard

parameter such as accuracy, precision, recall, and F1 score. The lines in this subfigure correspond to the baseline models, demonstrating their relative strengths and limitations.

In contrast, Fig. 8b showcases the performance metrics of the hybrid models using the same parameters. Exceptional performance for these metrics is reflected in the lines approaching the outer edges of the radar chart, highlighting the advantages of the hybrid models over the baseline. The separation into two subfigures allows for a more detailed and comparative visualisation of the model performances, emphasising the improvements achieved through the hybrid approach.

(1) Prediction of \mathcal{Y}_{HR} : A testing accuracy of 98.80% was achieved by the MLP model, with precision and recall rates of 100.00% and 94.79%, respectively. A testing accuracy of 100% was recorded for the XGBoost model. The MXBoost model achieved a testing accuracy of 98.80%, as depicted in Fig. 9a.

(2) Prediction of \mathcal{Y}_{SpO_2} : The MLP model recorded a testing accuracy of 98.90%, with precision and recall values of 100.00% and 95.31%, respectively. The XGBoost model demonstrated a testing accuracy of 100%. The MXBoost model reached a testing accuracy of 98.90%, as shown in Fig. 9b.

(3) Prediction of \mathcal{Y}_{BT} : A testing accuracy of 97.05% was registered for the MLP model, with precision and recall rates of 97.03% and 96.17%, respectively. A testing accuracy of 100% was observed in the XGBoost model. The MXBoost model achieved a testing accuracy of 98.50%, as illustrated in Fig. 9c.

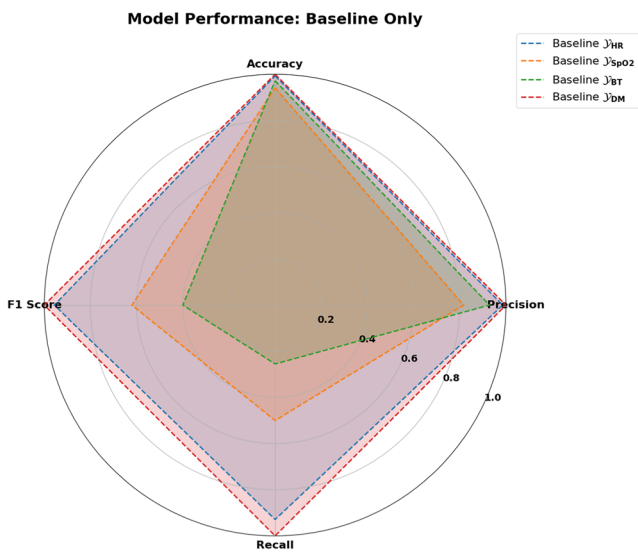
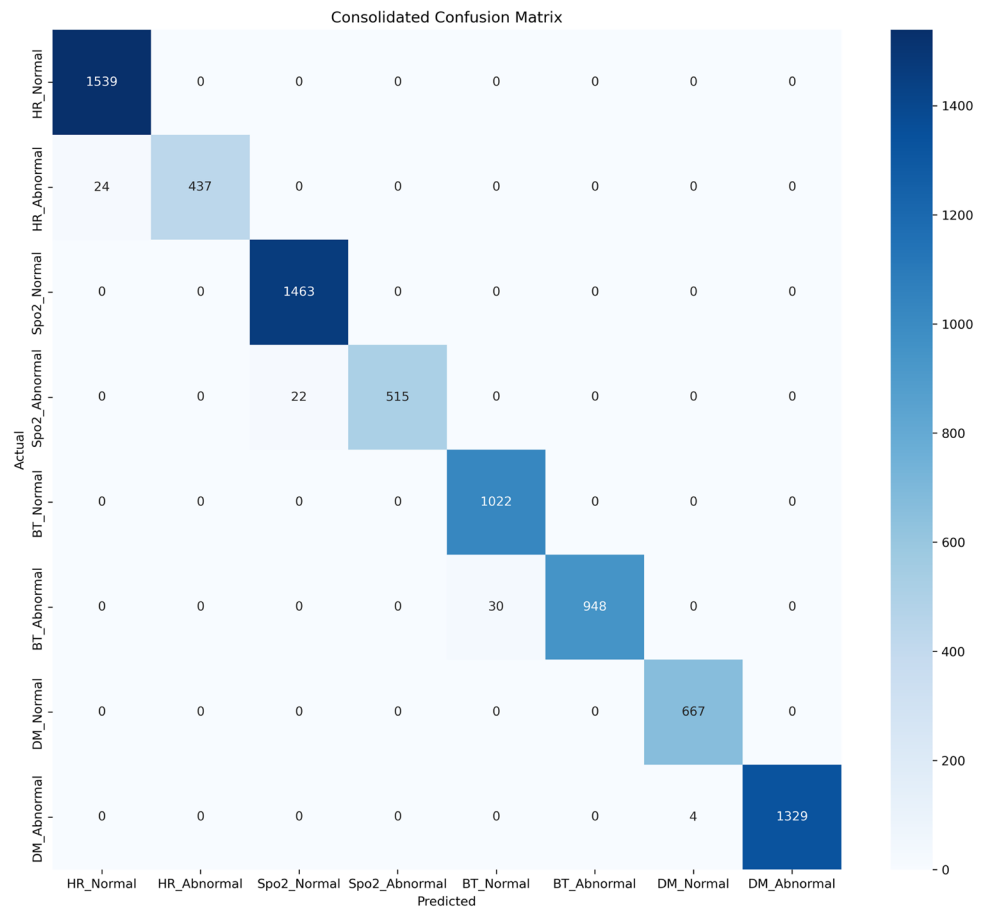
(4) Prediction of \mathcal{Y}_{DM} : A testing accuracy of 99.80% was recorded for the MLP model, with precision of 100% and recall of 99.54%. The XGBoost model exhibited a testing accuracy of 100%. The MXBoost model attained a testing accuracy of 99.80%, as presented in Fig. 9d.

(5) Macro Average Calculations: The macro average F1 score and the recall values were calculated to be 0.984 and 0.97, respectively. These metrics indicate exceptional performance across all classes.

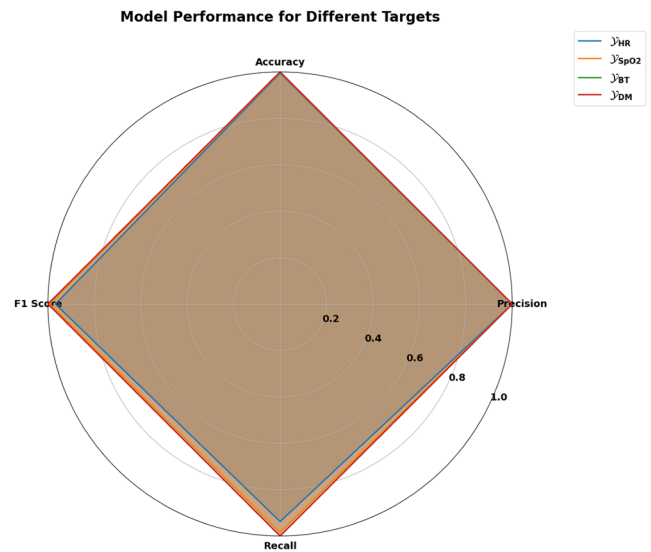
$$\text{Macro Avg} = \frac{1}{N} \sum_{i=1}^N \text{Metric}_i, \tag{16}$$

[57] where N is the number of classes, and Metric_i is the metric calculated for the i -th class.

Fig. 7 Heatmap of the confusion matrix for the hybrid model



(a) Baseline Performance Metrics.



(b) Hybrid Models Performance.

Fig. 8 Radar charts depicting performance metrics of the models. **a** Baseline model performance metrics. **b** Hybrid model performance metrics

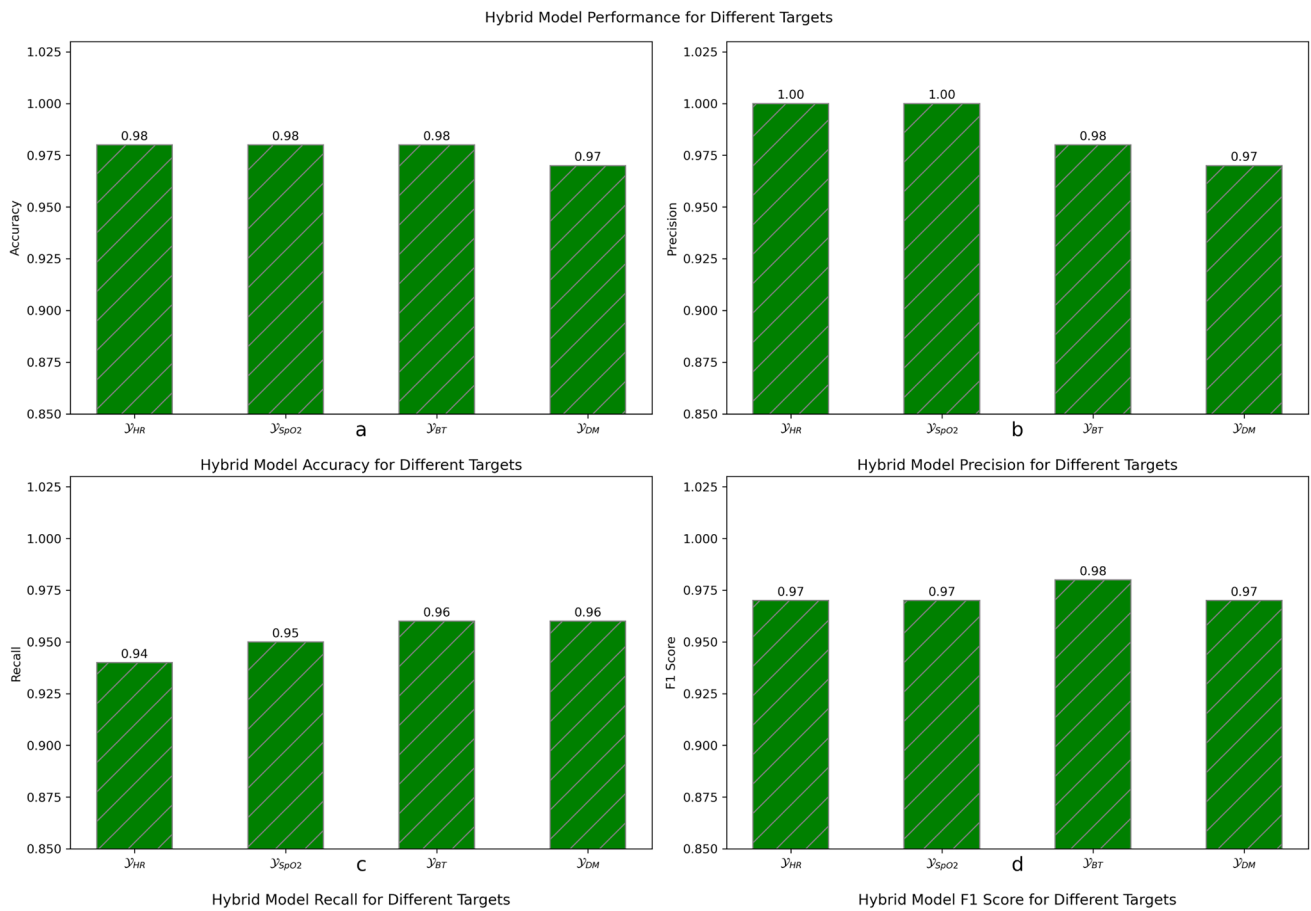


Fig. 9 Hybrid model performance

(6) Weighted Average Calculations: The weighted average F1-score and recall were found to be extremely high at 0.984 and 0.97, respectively.

$$\text{Weighted Avg} = \frac{1}{N} \sum_{i=1}^N w_i \cdot \text{Metric}_i, \quad (17)$$

[58] where w_i is the weight of the i -th class, and Metric_i is the metric calculated for the i -th class.

Table 5 reveals that both the macro and weighted averages are nearly identical, suggesting a balanced distribution among the classes, and thereby implying that each class has a comparable number of instances.

6.3 The distribution of prediction errors

The distribution of errors between predicted and actual values for the four targets (DM, HR, SpO2, and BT) is illustrated in Fig. 10. A concentration of errors around the zero line has been observed, indicating that a close alignment between the predictions and actual values was achieved by the hybrid model. This alignment demonstrates the robustness of the model. The autocorrelation plot, as depicted in Fig. 11, reveals temporal patterns in the discrepancies between predicted and actual values. Several observations can be made based on this visual representation:

(1) Statistical Significance: The level of confidence in the results of statistical analyses is represented by bands set at $\pm \frac{2}{\sqrt{N}}$, where N is the total number of occurrences. Correlation coefficients within these bands are considered statistically significant. The Eq.(18) was derived by [59].

Table 5 Performance metrics across different classes

| Metrics | Average type | Precision | Recall | F1-score |
|---------|--------------|-----------|--------|----------|
| HR | Macro Avg | 0.9923 | 0.9740 | 0.9828 |
| | Weighted Avg | 0.9882 | 0.9880 | 0.9879 |
| SpO2 | Macro Avg | 0.9926 | 0.9795 | 0.9858 |
| | Weighted Avg | 0.9892 | 0.9890 | 0.9889 |
| BT | Macro Avg | 0.9857 | 0.9847 | 0.9850 |
| | Weighted Avg | 0.9854 | 0.9850 | 0.9850 |
| DM | Macro Avg | 0.9970 | 0.9985 | 0.9978 |
| | Weighted Avg | 0.9980 | 0.9980 | 0.9980 |

$$\alpha = \pm \frac{2}{\sqrt{N}} \quad (18)$$

(2) Temporal Lag Interpretation: The concept of lag in data analysis is explained, wherein a lag of one compares data points with their immediate predecessors, and a lag of five compares data from five periods earlier. The autocorrelation related to lag k :

$$r_k = \frac{\sum_{i=k}^N (Y_t - \hat{Y})(Y_{t-k} - \hat{Y})}{\sum_{i=1}^N (Y_t - \hat{Y})^2}, \quad (19)$$

(3) Diminishing Autocorrelation: A decrease in autocorrelation values over time suggests a pattern in the data.

(4) Stochastic Fluctuations: Irregular peaks in the dataset may indicate a lack of a strong seasonal pattern, while repeated high points at regular intervals suggest a seasonal pattern.

(5) Negative Autocorrelation Phenomena: Instances where values above the mean are followed by values below the mean, and vice versa, are often observed. This is mathematically represented as $r_k < 0$.

Figure 11 shows that the actual differences and rolling average lines consistently intersect at zero, indicating that the model's predictions are both stable and objective over time. This consistent pattern suggests the absence of systematic errors in the model's predictions, thereby enhancing their reliability across the entire dataset. The analysis of more than 10,000 data points revealed synchronized behavior across various indices, further validating the robustness of the model.

6.4 Performance comparison of healthcare prediction models

A comparative analysis of the performance of several models, including our proposed work, is provided in the Table 6 in terms of accuracy, F1-score, precision, and response time. A superior balance between high accuracy (98.90%) and rapid response time (6 ms) is demonstrated by our model, indicating its suitability for real-time healthcare applications.

The other models exhibit varied performance metrics, with differences in response times and accuracy depending on the application. For instance, the model by Zhang and Jin demonstrates a faster response time of 0.25 s; however, its accuracy is lower at 81.90%. Similarly, the work of Manocha et al. focuses on health monitoring in rural areas with minimal delay, but the accuracy remains below that of our model.

6.5 Comparative analysis of digital twin applications in healthcare research

To contextualise the contributions and effectiveness of our approach, we present a comparative analysis with existing DT applications in healthcare. This comparison serves to highlight the unique aspects and advantages of our work and establish its position relative to current research in the field. The metrics and methodologies used for this comparison are aligned with those used in our evaluation, providing a direct basis for comparison.

Table 7 provided an analytical overview of various applications of DT technologies in healthcare. The objectives of these studies span a wide range of healthcare issues, from post-stroke rehabilitation [50] to type 1 diabetes management [9]. The research designs employed in these studies also vary. Some studies, such as [50] and [27], focus on frameworks and case

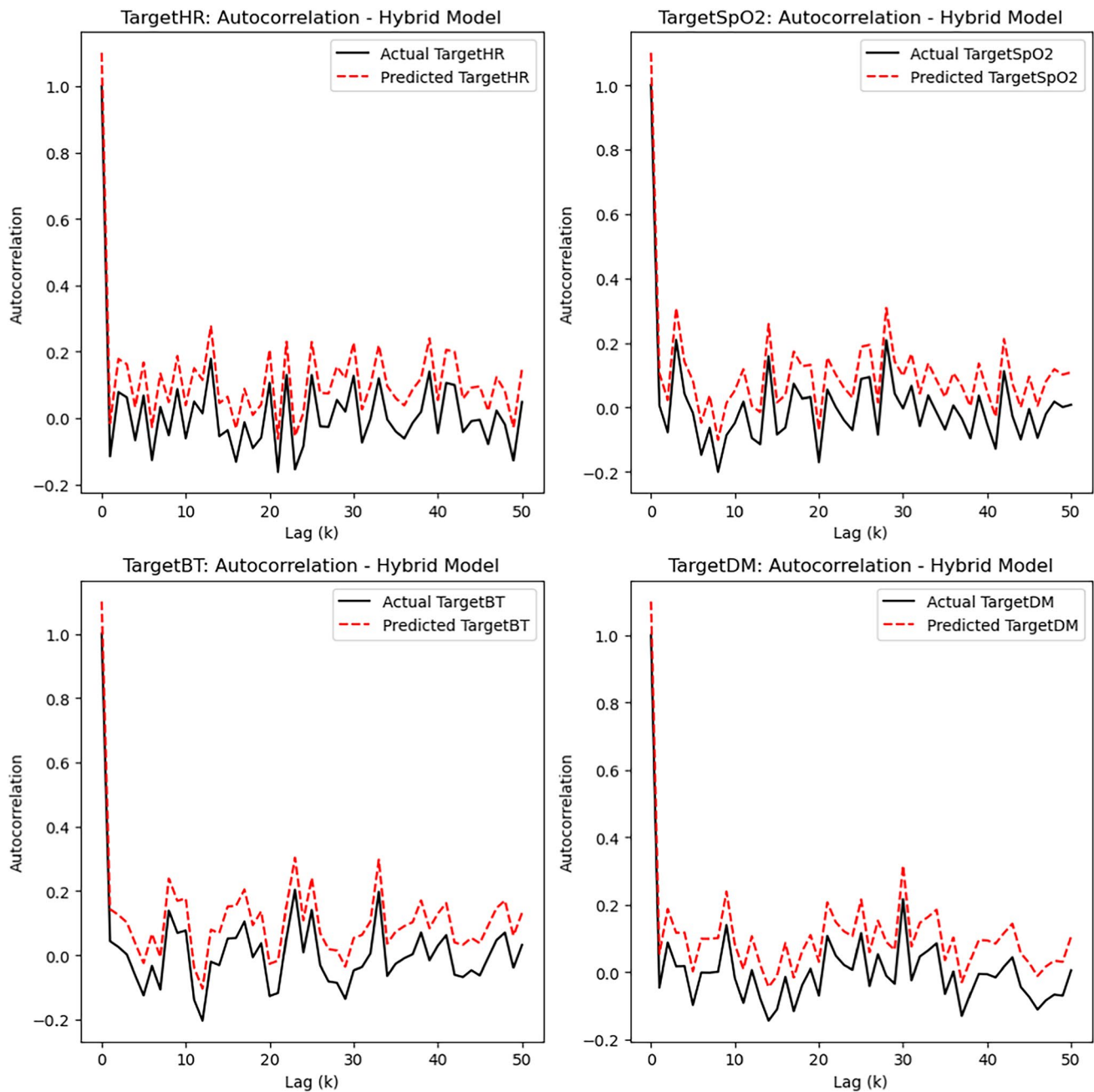


Fig. 10 Distribution of prediction errors for important health metrics

studies, while others, such as [46] emphasise architectural designs and mechanisms. The technological platforms used in these studies are diverse. For instance, cloud computing is used in [50] and [27], while blockchain technology is the focus of [46]. The methodologies for modelling also differ. Some studies employ traditional methods of DT and virtual reality (VR) [50], while others explore advanced techniques such as complex DT architectures and ML algorithms [25]. Validation methods are context-dependent. Real-world case studies are preferred in some research [50], while experimental settings and simulations are used in others, such as [41]. Our work distinguishes itself by integrating multiple technologies into a unified software platform, aiming to establish a comprehensive DT environment for healthcare. This integration allows for robust remote monitoring, diagnostics, predictive analytics, and security measures.

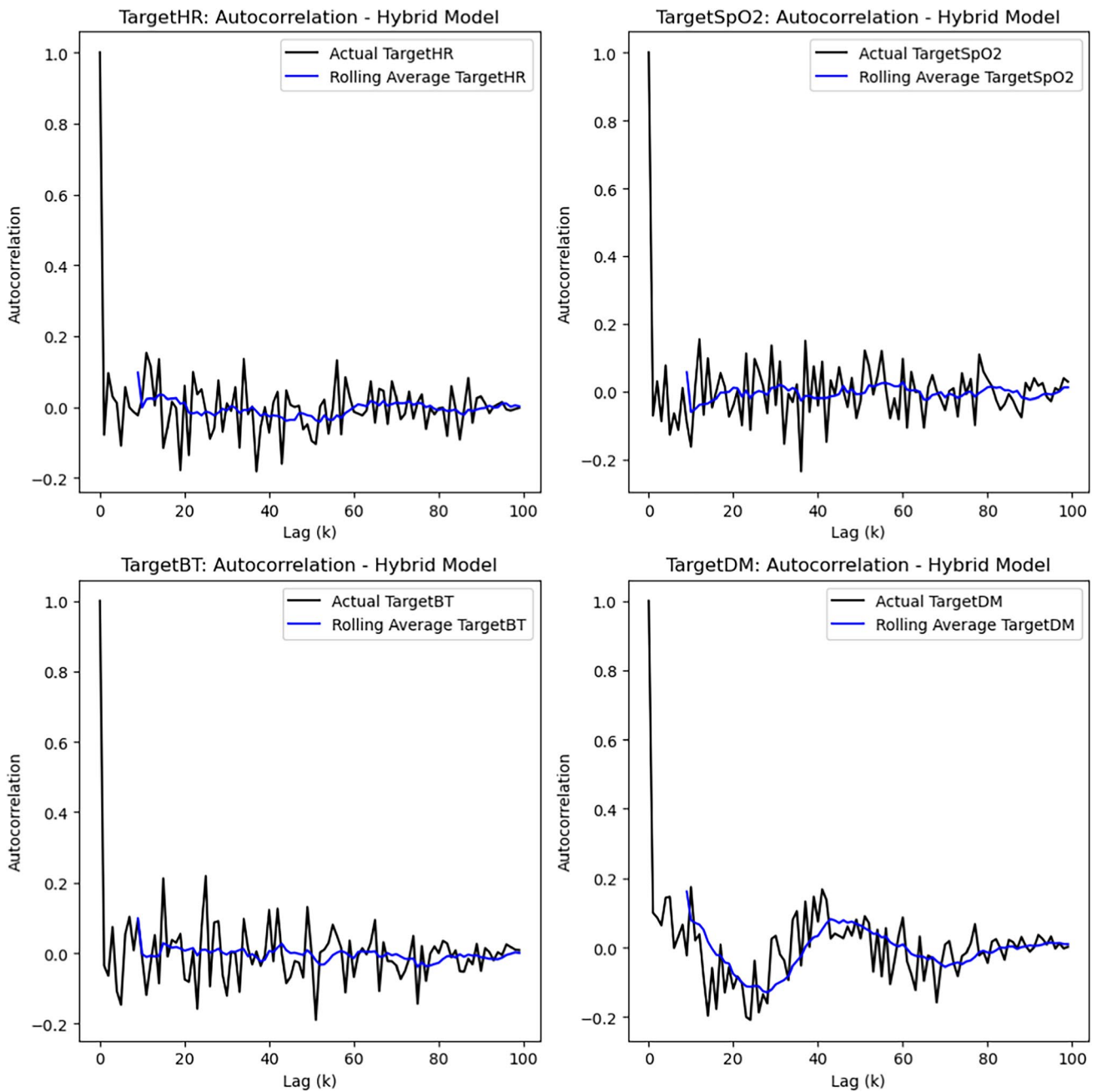


Fig. 11 Autocorrelation and Rolling Average of Prediction Errors for Important Health Metrics

Table 6 Performance Comparison of Different Models

| Model | Accuracy (%) | F1-score | Precision | Response time |
|----------|--------------|----------|-----------|---------------|
| Our work | 98.90 | 0.98 | 0.98 | 6 ms |
| [60] | 95.26 | 0.95 | 0.95 | 94.53s |
| [61] | 96.00 | 0.78 | 0.80 | N/A |
| [62] | 81.90 | 0.77 | 0.82 | 0.25s |
| [63] | 82.00 | 0.82 | 0.82 | N/A |
| [64] | 95.09 | 0.95 | 0.95 | Minimal Delay |

Table 7 Benchmarking DT applications in the healthcare environment

| Ref. no | Research design | Technology | \mathcal{M}_Q^a | Validation | Results |
|----------|--|---|------------------------------------|--|---|
| [50] | \mathcal{F}_A , C_Σ & C_Σ^d | Cloud Computing, VR, Unity | DT, VR, AI | Real-world C_Σ | Improved Rehabilitation via VR & DT |
| [27] | \mathcal{F}_A & C_Σ | Cloud Computing, Wearables | DTH Model | C_Σ | Real-time Supervision for Elderly |
| [29] | Scheme & C_Σ | Edge-centric \mathcal{F}_A | CSDR-DT Scheme | Simulation & C_Σ | More Accurate & Efficient DT |
| [41] | Algorithm Improvement & System Design | Tensorflow, Weka, Python, Linux | DT & DL | Exp. ^g | Improved Disease Recognition & Resource Sharing |
| [65] | Model Development & Prototype | Ramus, NN | DT of Consumer, NN | Prototype | Prototype for food personalisation |
| [25] | \mathcal{F}_A & Classifier | IoT, ML | DT, ML, NN | Classifier & \mathcal{F}_A | Improved Heart Disease Monitoring |
| [26] | \mathcal{F}_A & AI Model | AI, GAN ^b | DT, AI, GAN | AI Model & \mathcal{F}_A | Improved Chronic Wound Care |
| [44] | Literature Review, Architecture & C_Σ | Architecture, CanTwin | Six-layer DT Structure | C_Σ (CanTwin) | Social Distancing & People Flow Management |
| [45] | \mathcal{F}_A & Exp. ^g | GANs, RNNs | GAN \mathcal{F}_A (GluGAN) | Clinical Datasets & Exp. ^g | Data-driven Decision Support in T1D |
| [33] | \mathcal{F}_A & Clinical Trials | IoT, DTH, LB-MPC, Python | DTH, DL, LB-MPC | Clinical Trials & Simulations | Improved Time-in-Range, Reduced Insulin Infusion |
| [34] | \mathcal{F}_A & Prototyping | Raspberry Pi, 3-D Modelling | DT, 3-D Models | To be conducted | Interactive Functionality, Comfort |
| [9] | \mathcal{F}_A & Simulation | Custom \mathcal{F}_A , Bayesian Parameter Estimation | DT, Nonlinear Physiological Models | Simulated Data & Two Real-world C_Σ | High Accuracy in Simulating Different Treatment Scenarios |
| Our work | \mathcal{F}_A , dashboard, and Exp. ^g | Cloud Computing, Json, Python, ML, DL, IoT, Arduino IDE | DTH Model, AI | C_Σ | Integrating multiple technologies into a single software platform to establish a unified DT environment for healthcare. |

^a Modelling Methodology; ^b Generative Adversarial Network; ^c Framework; ^d Case Study; ^e Elderly Type 2 Diabetes; ^f Type 1 Diabetes; ^g Experiments Case

7 Discussion

7.1 Potential impact on healthcare

The integration of IoT devices, cloud computing, and ML models has demonstrated the potential to revolutionise patient care. Real-time monitoring systems can significantly improve the early detection of health abnormalities, enabling timely medical interventions. This capability is especially critical for conditions that require immediate attention, such as hypoxia or severe hyperglycemia in diabetic patients. Additionally, remote monitoring and telemedicine services can be facilitated, making healthcare more accessible to underserved populations.

7.2 Challenges of the study

A notable challenge in this study arises from the complexity of integrating multiple programming platforms and languages to establish a unified digital twin environment. The system relies on a multidisciplinary approach, i.e., the Arduino IDE for sensor interfacing, Python for data processing, C# for cloud operations, and JSON formats for data transmission. While each platform's strengths are utilised, the difficulty of achieving compatibility across systems has been recognised, along with the increased burden of development and maintenance. Furthermore, robust security measures must be ensured across these diverse technologies, especially given the sensitive nature of health data in remote monitoring applications. Future iterations may focus on streamlining the integration process, possibly by adopting a more uniform development environment or by creating custom middleware to bridge the different platforms. Despite measures taken to protect patient data, the growing prevalence of cyber threats continues to present a significant concern. Future research should be directed towards expanding the prediction model to include genetic markers or lifestyle factors unique to individual patients. Continued refinement of security measures will also be necessary to protect against evolving cyber threats. Additionally, further integration with existing healthcare systems and long-term validation studies should be pursued.

8 Conclusion

The aim of this study was to address the challenges of real-time healthcare monitoring by developing a comprehensive architecture for digital twins within situationally aware healthcare systems. The key contribution of this work is the seamless integration of IoT for real-time data collection, cloud computing for scalable data processing, and advanced algorithms for accurate health predictions. This integration was realised through both physical and digital architectures, encompassing sensing equipment, real-time data synthesis, cloud-based storage, multi-objective algorithms, and intuitive dashboard analytics.

High accuracy in predicting critical health indices, e.g., HR, SpO₂, BT, and DM, was achieved in real time using MXBoost, a hybrid model designed to manage multiple targets and large data volumes. This model, which combines the MLP and XGBoost algorithms, led to a 25.6% increase in processing speed, 98.9% procedural robustness, and an F1 score of 0.984. Under noisy conditions, a real-time accuracy of 95.45% was recorded.

This study offers an integrated and adaptable approach to healthcare monitoring, setting a new standard for the incorporation of digital twins, IoT, and advanced algorithms in healthcare systems. Additionally, autocorrelation and rolling analysis were employed to test prediction verification, stochastic fluctuations, and the distribution of prediction errors for key health metrics.

In future, the aspects of healthcare system designs can include the use of quantum computing for increase data security. Likewise, federated learning methods may support secure and decentralized management of health data across institutions. These advancements are expected to improve privacy protections while also enabling better scalability for large-scale systems in real time.

Acknowledgements The authors would like to acknowledge the support of Brunel University London for providing the necessary resources and facilities for this research.

Author contributions Ahmed K. Jameil contributed to the conceptualisation, design, data acquisition, analysis, and interpretation. He developed the methodology, provided resources, validated results, and drafted the manuscript. Hamed Al Raweshidy oversaw funding acquisition, investigation, project management, and supervision. He provided resources and critically revised the manuscript. Both authors are accountable for the accuracy and integrity of the work.

Funding This research was supported by Brunel University London.

Data availability Data is available on request from the authors.

Declarations

Ethics approval and consent to participate The study was conducted in accordance with the ethical guidelines of Brunel University London. A risk assessment was performed, and the study protocol was reviewed and approved by the University's Ethics Committee. Informed consent was obtained from all 20 participants who were continuously monitored for key physiological parameters (e.g., heart rate, oxygen saturation levels, body temperature). Additionally, the study adhered to the General Data Protection Regulation (GDPR) and the Declaration of Helsinki. To supplement the data collected from the 20 participants and enhance diversity, the MIMIC-III Public Health Dataset was utilized. This publicly available and anonymized dataset in accordance with applicable data protection regulations [30]. The dataset is accessible at <https://mimic.physionet.org/>.

Consent for publication As this study utilized anonymized data from a public dataset, informed consent was waived. The dataset complies with the relevant data protection and privacy regulations.

Competing interests The authors declare no competing interests.

Open Access This article is licensed under a Creative Commons Attribution 4.0 International License, which permits use, sharing, adaptation, distribution and reproduction in any medium or format, as long as you give appropriate credit to the original author(s) and the source, provide a link to the Creative Commons licence, and indicate if changes were made. The images or other third party material in this article are included in the article's Creative Commons licence, unless indicated otherwise in a credit line to the material. If material is not included in the article's Creative Commons licence and your intended use is not permitted by statutory regulation or exceeds the permitted use, you will need to obtain permission directly from the copyright holder. To view a copy of this licence, visit <http://creativecommons.org/licenses/by/4.0/>.

References

1. Attaran M, Celik BG. Digital twin: benefits, use cases, challenges, and opportunities. *Decis Anal J*. 2023;6: 100165. <https://doi.org/10.1016/j.dajour.2023.100165>.
2. Fernandez-Ruiz I. Computer modelling to personalize bioengineered heart valves. *Nat Rev Cardiol*. 2018;15(8):440–1. <https://doi.org/10.1038/s41569-018-0040-x>.
3. Grieves M. Digital twin : manufacturing excellence through virtual factory replication. White Pap. 2014;1:1–7.
4. Chu Y, Li S, Tang J, Wu H. The potential of the medical digital twin in diabetes management: a review. *Front Med*. 2023. <https://doi.org/10.3389/fmed.2023.1178912>.
5. Mohamed N, Al-Jaroodi J, Jawhar I, Kesserwan N. Leveraging digital twins for healthcare systems engineering. *IEEE Access*. 2023;11:69841–53. <https://doi.org/10.1109/access.2023.3292119>.
6. Singh M, Fuenmayor E, Hinchy EP, Qiao Y, Murray N, Devine D. Digital twin: origin to future. *Appl Syst Innov*. 2021;4(2):36.
7. Jimenez JI, Jahankhani H, Kendzierskyj S. Health care in the cyberspace: medical cyber-physical system and Digital Twin challenges. *Digital Twin technologies and smart cities*. Singapore: Springer; 2020. p. 79–92.
8. Yousefvand A, Jameil AK, Abbas YA, Meshginqalam B, Ahmadi MT. The effect of uniaxial strain on the electrical properties of graphene nanoribbon. In: 2018 1st international scientific conference of engineering sciences - 3rd scientific conference of engineering science (ISCES), 2018; <https://doi.org/10.1109/ISCES.2018.8340525>
9. Cappon G, Vettoretti M, Sparacino G, Favero SD, Facchinetti A. Replaybg: a digital twin-based methodology to identify a personalized model from type 1 diabetes data and simulate glucose concentrations to assess alternative therapies. *IEEE Trans Biomed Engin*. 2023. <https://doi.org/10.1109/tbme.2023.3286856>.
10. Makam S, Komatineni BK, Meena SS, Meena U. Unmanned aerial vehicles (uavs): an adoptable technology for precise and smart farming. *Discov Internet Thing*. 2024;4(1):12. <https://doi.org/10.1007/s43926-024-00066-5>.
11. Jameil AK, Al-Raweshidy H. Ai-enabled healthcare and enhanced computational resource management with digital twins into task offloading strategies. *IEEE Access*. 2024;12:90353–70. <https://doi.org/10.1109/ACCESS.2024.3420741>.
12. Khan S, Arslan T, Ratnarajah T. Digital twin perspective of fourth industrial and healthcare revolution. *IEEE Access*. 2022;10:25732–54.
13. Jameil AK, Al-Raweshidy H. Implementation and Evaluation of Digital Twin Framework for Internet of Things Based Healthcare Systems. *IET Wireless Sensor Systems TBA(TBA)*, 2024. <https://doi.org/10.1049/wss2.12101> . In Production
14. Bryson G, O'Dwyer D. Benefits and challenges of digital pathology use for primary diagnosis in gynaecological practice: a real-life experience. *Diagn Histopathol*. 2023. <https://doi.org/10.1016/j.jmpdhp.2023.07.001>.

15. Jameil AK, Al-Raweshidy H. Enhancing offloading with cybersecurity in edge computing for digital twin-driven patient monitoring. *IET Wirel Sen Syst*. 2024. <https://doi.org/10.1049/wss2.12086>.
16. Munyao MM, Maina EM, Mambo SM, Wanyoro A. Real-time pre-eclampsia prediction model based on IoT and machine learning. *Discov Int Thing*. 2024;4(1):10. <https://doi.org/10.1007/s43926-024-00063-8>.
17. Al-Sadoon ME, Jedidi A, Al-Raweshidy H. Dual-tier cluster-based routing in mobile wireless sensor network for IoT application. *IEEE Access*. 2023;11:4079–94. <https://doi.org/10.1109/ACCESS.2023.3235200>.
18. Gopichand G, Sarath T, Dumka A, Goyal HR, Singh R, Gehlot A, Gupta LR, Thakur AK, Priyadarshi N, Twala B. Use of IoT sensor devices for efficient management of healthcare systems: a review. *Discov Int Thing*. 2024;4(1):8. <https://doi.org/10.1007/s43926-024-00062-9>.
19. Rodrigues VF, Rosa Righi R, Costa CA, Zeiser FA, Eskofier B, Maier A, Kim D. Digital health in smart cities: rethinking the remote health monitoring architecture on combining edge, fog, and cloud. *Health Technol*. 2023;13(3):449–72.
20. Jameil AK, Al-Raweshidy H. Efficient cnn architecture on fpga using high level module for healthcare devices. *IEEE Access*. 2022;10:60486–95. <https://doi.org/10.1109/ACCESS.2022.3180829>.
21. Aceto G, Persico V, Pescapé A. Industry 4.0 and health: internet of things, big data, and cloud computing for healthcare 4.0. *J Indust Inf Int*. 2020;18:100129. <https://doi.org/10.1016/j.jii.2020.100129>.
22. Jameil AK, Al-Raweshidy H. Hybrid Cloud-Edge AI framework for Real-Time predictive analytics in Digital Twin healthcare systems. *Research Square* 2024. <https://doi.org/10.21203/rs.3.rs-5412158/v1>.
23. Feng Y, Zhao J, Chen X, Lin J. An in silico subject-variability study of upper airway morphological influence on the airflow regime in a tracheobronchial tree. *Bioengineering*. 2017;4(4):90. <https://doi.org/10.3390/bioengineering4040090>.
24. Al-Janabi TA, Al-Raweshidy HS. An energy efficient hybrid mac protocol with dynamic sleep-based scheduling for high density IoT networks. *IEEE Int Thing J*. 2019;6(2):2273–87. <https://doi.org/10.1109/JIOT.2019.2905952>.
25. Elayan H, Aloqaily M, Guizani M. Digital twin for intelligent context-aware IoT healthcare systems. *IEEE Int Thing J*. 2021;8(23):16749–57. <https://doi.org/10.1109/jiot.2021.3051158>.
26. Sarp S, Kuzlu M, Zhao Y, Gueler O. Digital twin in healthcare: a study for chronic wound management. *IEEE J Biomed Health Inf*. 2023. <https://doi.org/10.1109/jbhi.2023.3299028>.
27. Liu Y, Zhang L, Yang Y, Zhou L, Ren L, Wang F, Liu R, Pang Z, Deen MJ. A novel cloud-based framework for the elderly healthcare services using digital twin. *IEEE Access*. 2019;7:49088–101.
28. Menon D, Anand B, Chowdhary CL. Digital twin: exploring the intersection of virtual and physical worlds. *IEEE Access*. 2023;11:75152–72. <https://doi.org/10.1109/access.2023.3294985>.
29. Jia P, Wang X, Shen X. Accurate and efficient digital twin construction using concurrent end-to-end synchronization and multi-attribute data resampling. *IEEE Int Thing J*. 2022;10(6):4857–70.
30. Das C, Mumu AA, Ali MF, Sarker SK, Mueen SM, Das SK, Das P, Hasan MM, Tasneem Z, Islam MM, Islam MR, Badal FR, Ahamed MH, Abhi SH. Toward iort collaborative digital twin technology enabled future surgical sector: technical innovations, opportunities and challenges. *IEEE Access*. 2022;10:129079–104. <https://doi.org/10.1109/access.2022.3227644>.
31. Corral-Acero J, Margara F, Marciniak M, Rodero C, Loncaric F, Feng Y, Gilbert A, Fernandes JF, Bukhari HA, Wajdan A, et al. The ‘digital twin’ to enable the vision of precision cardiology. *Eur Heart J*. 2020;41(48):4556–64.
32. Zhang J, Li L, Lin G, Fang D, Tai Y, Huang J. Cyber resilience in healthcare digital twin on lung cancer. *IEEE Access*. 2020;8:201900–13. <https://doi.org/10.1109/access.2020.3034324>.
33. Thamotharan P, Srinivasan S, Kesavadev J, Krishnan G, Mohan V, Seshadhri S, Bekiroglu K, Toffanin C. Human digital twin for personalized elderly type 2 diabetes management. *J Clin Med*. 2023;12(6):2094.
34. Yu F, Chen Z, Jiang M, Tian Z, Peng T, Hu X. Smart clothing system with multiple sensors based on digital twin technology. *IEEE Int Thing J*. 2022;10(7):6377–87.
35. Altamimi S, Abu Al-Haija Q. Maximizing intrusion detection efficiency for IoT networks using extreme learning machine. *Discov Int Thing*. 2024;4(1):5. <https://doi.org/10.1007/s43926-024-00060-x>.
36. Al-Kaseem BR, Al-Raweshidy HS. Sd-nfv as an energy efficient approach for m2m networks using cloud-based 6lowpan testbed. *IEEE Int Thing J*. 2017;4(5):1787–97. <https://doi.org/10.1109/JIOT.2017.2704921>.
37. Panahi M, Masihi S, Hanson AJ, Rodriguez-Labra JI, Masihi A, Maddipatla D, Narakathu BB, Lawson D, Atashbar MZ. Development of a flexible smart wearable oximeter insole for monitoring spo2 levels of diabetics’ foot ulcer. *IEEE J Flex Electron*. 2023;2(2):61–70. <https://doi.org/10.1109/jflex.2022.3232465>.
38. Rajesh KNVPS, Dhuli R. Classification of imbalanced ecg beats using re-sampling techniques and adaboost ensemble classifier. *Biomed Signal Process Control*. 2018;41:242–54. <https://doi.org/10.1016/j.bspc.2017.12.004>.
39. Mondejar-Guerra V, Novo J, Rouco J, Penedo MG, Ortega M. Heartbeat classification fusing temporal and morphological information of ecgs via ensemble of classifiers. *Biomed Signal Process Control*. 2019;47:41–8. <https://doi.org/10.1016/j.bspc.2018.08.007>.
40. Vaskovsky AM, Chvanova MS. Designing the neural network for personalization of food products for persons with genetic president of diabetic sugar. In: 2019 3rd school on dynamics of complex networks and their application in intellectual robotics (DCNAIR), IEEE: New York. 2019; pp. 175–177.
41. Lv Z, Guo J, Lv H. Deep learning-empowered clinical big data analytics in healthcare digital twins. *IEEE ACM Trans Comput Biol Bioinform*. 2023. <https://doi.org/10.1109/tcbb.2023.3252668>.
42. Khan M, Hatami M, Zhao W, Chen Y. A novel trusted hardware-based scalable security framework for IoT edge devices. *Discov Int Thing*. 2024;4(1):4. <https://doi.org/10.1007/s43926-024-00056-7>.
43. Kocabas O, Soyata T, Aktas MK. Emerging security mechanisms for medical cyber physical systems. *IEEE/ACM Trans Comput Biol Bioinform*. 2016;13(3):401–16. <https://doi.org/10.1109/tcbb.2016.2520933>.
44. De Benedictis A, Mazzocca N, Somma A, Strigaro C. Digital Twins in healthcare: an architectural proposal and its application in a social distancing case study. *IEEE J Biomed Health Inform*. 2022;10(7):6377–87.
45. Zhu T, Li K, Herrero P, Georgiou P, Glugan: generating personalized glucose time series using generative adversarial networks. *IEEE J Biomed Health Inform*. 2023. <https://doi.org/10.1109/jbhi.2023.3271615>.

46. Lin Y, Gao Z, Shi W, Wang Q, Li H, Wang M, Yang Y, Rui L. A novel architecture combining oracle with decentralized learning for IIoT. *IEEE Int Thing J*. 2022. 10(5):3774–85.
47. Asghari A, Sohrabi MK. Server placement in mobile cloud computing: a comprehensive survey for edge computing, fog computing and cloudlet. *Comput Sci Rev*. 2024;51: 100616. <https://doi.org/10.1016/j.cosrev.2023.100616>.
48. Hajar MS, Al-Kadri MO, Kalutarage HK. A survey on wireless body area networks: architecture, security challenges and research opportunities. *Comput Sec*. 2021;104: 102211. <https://doi.org/10.1016/j.cose.2021.102211>.
49. Aghdam ZN, Rahmani AM, Hosseinzadeh M. The role of the internet of things in healthcare: future trends and challenges. *Comput Method Progr Biomed*. 2021;199: 105903. <https://doi.org/10.1016/j.cmpb.2020.105903>.
50. Zhong Y, Marteau B, Hornback A, Zhu Y, Shi W, Giuste F, Krzak JJ, Graf A, Chafetz R, Wang MD. IDTVR: a novel cloud framework for an interactive digital twin in virtual reality. In: 2022 IEEE 2nd international conference on intelligent reality (ICIR), IEEE: New York. 2022;pp. 21–26.
51. Althubaiti A. Sample size determination: a practical guide for health researchers. *J Gen Fam Med*. 2023;24(2):72–8.
52. Ashfaq Z, Mumtaz R, Rafay A, Zaidi SMH, Saleem H, Mumtaz S, Shahid A, Poorter ED, Moerman I. Embedded ai-based digi-healthcare. *Appl Sci*. 2022;12(1):519. <https://doi.org/10.3390/app12010519>.
53. Bruce S. Applied cryptography: protocols, algorithms, and source code in C.-2nd. Hoboken: John Wiley & Sons; 1996.
54. Rivest RL, Shamir A, Adleman L. A method for obtaining digital signatures and public-key cryptosystems. *Commun ACM*. 1978;21(2):120–6.
55. Tiburski RT, Amaral LA, De Matos E, De Azevedo DF, Hessel F. The role of lightweight approaches towards the standardization of a security architecture for IoT middleware systems. *IEEE Commun Mag*. 2016;54(12):56–62.
56. Zahra SR, Chishti MA. Ransomware and internet of things: a new security nightmare. In: 2019 9th international conference on cloud computing, data science & engineering (confluence). IEEE. 2019; pp. 551–555.
57. Hotelling H. The generalization of student's t-test to correlated samples. *Biometrika*. 1935;24(3/4):321–78.
58. Hoche R. Nicomachi geraseni pythagorei introductionis arithmeticae libri II. B. G. Teubner, Leipzig. 1866. <https://archive.org/details/arithmetica00nicougoog>.
59. Cohen J. Statistical power analysis for the behavioral sciences. 2nd ed. Hillsdale: Lawrence Erlbaum Associates; 1994.
60. Kumar D, Sood SK, Rawat KS. Early health prediction framework using xgboost ensemble algorithm in intelligent environment. *Artif Int Rev*. 2023;56(S1):1591–615. <https://doi.org/10.1007/s10462-023-10565-6>.
61. Bopche R, Gustad LT, Afset JE, Ehrnstrm B, Damas JK, Nytro O. In-hospital mortality, readmission, and prolonged length of stay risk prediction leveraging historical electronic patient records. *JAMIA Open*. 2024;7(3):074. <https://doi.org/10.1093/jamiaopen/ooae074>.
62. Zhang J, Jin Z, Tang B, Huang X, Wang Z, Chen Q, He J. Enhancing trauma care: a machine learning approach with xgboost for predicting urgent hemorrhage interventions using ntdb data. *Bioengineering*. 2024;11(8):768. <https://doi.org/10.3390/bioengineering11080768>.
63. Li Y, Du C, Ge S, Zhang R, Shao Y, Chen K, Li Z, Ma F. Hematoma expansion prediction based on smote and xgboost algorithm. *BMC Med Inf Decis Mak*. 2024;24(1):172. <https://doi.org/10.1186/s12911-024-02561-9>.
64. Manocha A, Sood SK, Bhatia M. lot-dew computing-inspired real-time monitoring of indoor environment for irregular health prediction. *IEEE Trans Engin Manag*. 2024;71:1669–82. <https://doi.org/10.1109/TEM.2023.3338458>.
65. Vaskovsky AM, Chvanova MS, Rebezov MB. Creation of digital twins of neural network technology of personalization of food products for diabetics. In: 2020 4th 4th scientific school on dynamics of complex networks and their application in intellectual robotics (DCNAIR), IEEE: New York. 2020; pp. 251–253.

Publisher's Note Springer Nature remains neutral with regard to jurisdictional claims in published maps and institutional affiliations.